

# Informed proposals for local MCMC in discrete spaces

Giacomo Zanella

February 18, 2022

## Abstract

There is a lack of methodological results to design efficient Markov chain Monte Carlo (MCMC) algorithms for statistical models with discrete-valued high-dimensional parameters. Motivated by this consideration, we propose a simple framework for the design of informed MCMC proposals (i.e. Metropolis-Hastings proposal distributions that appropriately incorporate local information about the target) which is naturally applicable to both discrete and continuous spaces. We explicitly characterize the class of optimal proposal distributions under this framework, which we refer to as *locally-balanced* proposals, and prove their Peskun-optimality in high-dimensional regimes. The resulting algorithms are straightforward to implement in discrete spaces and provide orders of magnitude improvements in efficiency compared to alternative MCMC schemes, including discrete versions of Hamiltonian Monte Carlo. Simulations are performed with both simulated and real datasets, including a detailed application to Bayesian record linkage. A direct connection with gradient-based MCMC suggests that locally-balanced proposals may be seen as a natural way to extend the latter to discrete spaces.

## 1 Introduction

Markov chain Monte Carlo (MCMC) algorithms are one the most widely used methodologies to sample from complex and intractable probability distributions, especially in the context of Bayesian statistics [Robert and Casella, 2005]. Given a distribution of interest  $\Pi(dx)$  defined on some measurable space  $\mathcal{X}$ , MCMC methods simulate a Markov chain  $\{X_t\}_{t=1}^\infty$  having  $\Pi$  as stationary distribution and then use the states visited by  $X_t$  as Monte Carlo samples from  $\Pi$ . Under mild assumptions, the Ergodic Theorem guarantees that the resulting sample averages are consistent estimators for arbitrary expectations under  $\Pi$ . Many MCMC schemes used in practice fall within the Metropolis-Hastings (MH) framework [Metropolis et al., 1953, Hastings, 1970]. Given a current state  $x \in \mathcal{X}$ , the MH algorithm samples a proposed state  $y$  according to some proposal distribution  $Q(x, \cdot)$  and then accepts it with probability  $a(x, y) = \min \left\{ 1, \frac{\Pi(dy)Q(y, dx)}{\Pi(dx)Q(x, dy)} \right\}$  or otherwise rejects it and stays at  $x$ . The resulting transition kernel

$$P(x, dy) = Q(x, dy) + \delta_x(dy) \int_{\mathcal{X}} (1 - a(x, z)) Q(x, dz)$$

is  $\Pi$ -reversible and can be used for MCMC purposes. Although the MH algorithm can be applied to virtually any target distribution, its efficiency depends drastically on the proposal distribution  $Q$  and its interaction with the target  $\Pi$ . Good choices of  $Q$  will speed up the Markov chain's convergence while bad choices will slow it down in a potentially dramatic way.

**1.1 Random walk versus informed schemes** Random walk MH schemes use symmetric proposal distributions satisfying  $Q(x, y) = Q(y, x)$ , such as normal distributions centered at the current location  $Q_\sigma(x, \cdot) = N(x, \sigma^2 \mathbb{I}_n)$ . Although these schemes are easy to implement, the new state  $y$  is proposed “blindly” (i.e. using no information about  $\Pi$ ) and this can lead to bad mixing and slow convergence. In continuous frameworks, such as  $\mathcal{X} = \mathbb{R}^n$  and  $\Pi(dx) = \pi(x)dx$ , various *informed* MH proposal distributions have been designed to obtain better convergence. For example the Metropolis-Adjusted Langevin Algorithm (MALA, e.g. Roberts and Rosenthal, 1998) exploits the gradient of the target to bias the proposal distribution towards high probability regions by setting  $Q_\sigma(x, \cdot) = N(x + \frac{\sigma^2}{2} \nabla(\log \pi)(x), \sigma^2 \mathbb{I}_n)$ . Such an algorithm is derived by discretizing the  $\Pi$ -reversible Langevin diffusion  $X_t$  given by  $dX_t = \frac{\sigma^2}{2} \nabla(\log \pi)(x)dt + \sigma dB_t$ , so that the proposal  $Q_\sigma$  is approximately  $\Pi$ -reversible for small values of  $\sigma$ . More elaborate gradient-based informed proposals have been devised, such as Hamiltonian Monte Carlo (HMC, e.g. Neal [2011], Girolami and Calderhead [2011]), and other schemes [Welling and Teh, 2011, Titsias and Papaspiliopoulos, 2016, Durmus et al., 2017], resulting in substantial improvements of MCMC performances both in theory and in practice. However, most of these proposal distributions are derived as discretization of continuous-time diffusion processes or measure-preserving flows, and are based on derivatives and Gaussian distributions. Currently, it is not clear how to appropriately extend such methods to frameworks where  $\mathcal{X}$  is a discrete space. As a consequence, practitioners using MCMC to target measures on discrete spaces often rely on symmetric/uninformed proposal distributions, which can induce slow convergence.

**1.2 Informed proposals in discrete spaces** A simple way to circumvent the problem described above is to map discrete spaces to continuous ones and then apply informed schemes in the latter, typically using HMC [Zhang et al., 2012, Pakman and Paninski, 2013, Nishimura et al., 2017]. Although useful in some scenarios, the main limitation of this approach is that the embedding of discrete spaces into continuous ones is not always feasible and can potentially destroy the natural topological structure of the discrete space under consideration (e.g. spaces of trees, partitions, permutations, . . . ), thus resulting in highly multimodal and irregular target distributions that are hard to explore. An alternative approach was recently proposed in [Titsias and Yau, 2017], where informed proposals are obtained by introducing auxiliary variables and performing Gibbs Sampling in the augmented space. The resulting scheme, named the Hamming Ball sampler, requires no continuous space embedding and is directly applicable to generic discrete spaces, but the potentially strong correlation between the auxiliary variables and the chain state can severely slow down convergence.

In this work we formulate the problem of designing informed MH proposal distributions in an original way. Our formulation has the merit of being simple and unifying continuous and discrete frameworks. The theoretical results hint to a simple and practical class of informed MH proposal distributions that are well designed for high-dimensional discrete problems, which we refer to as *locally-balanced proposals*. Experiments on both simulated and real data show orders of magnitude improvements in efficiency compared to both random walk MH and the alternative informed schemes described above.

**1.3 Paper structure** In Section 2 we define the class of informed proposals distribution considered (obtained as a product of some “base” uninformed kernel and a biasing multiplicative term) and we characterize the class of biasing terms that are asymptotically-exact in the local limit regime (i.e. stepsize of the proposal going to 0). In Section 3 we show that, under regularity assumptions on the target, the same class of locally-balanced proposals is

also optimal in terms of Peskun ordering as the dimensionality of the state space increases. In Section 4 we consider a simple binary target distribution in order to compare different locally-balanced proposals and identify the one leading to the smallest mixing time, which turns out to be related to the Barker’s algorithm [Barker, 1965]. Section 5 discusses the connection with classical gradient-based MCMC and MALA in particular. In Section 6 we perform simulation studies on classic discrete models (permutation spaces and Ising model), while in Section 7 we consider a more detailed application to Bayesian Record Linkage problems. Finally, in Section 8 we discuss possible extensions and future works. Supplementary material includes proofs and additional details on the simulations studies.

## 2 Locally-balanced proposals

Let  $\Pi$  be a target probability distribution on some topological space  $\mathcal{X}$ . We assume that  $\Pi$  admits bounded density  $\pi$  with respect to some reference measure  $dx$ , meaning  $\Pi(dx) = \pi(x)dx$ . Typically  $dx$  would be the counting measure if  $\mathcal{X}$  is discrete or the Lebesgue measure if  $\mathcal{X} = \mathbb{R}^n$  for some  $n \geq 1$ .

Let  $K_\sigma(x, dy)$  be the uninformed symmetric kernel that we would use to generate proposals in a random walk MH scheme, such as a Gaussian distribution for continuous spaces or the uniform distribution over neighbouring states for discrete spaces. Here  $\sigma$  is a scale parameter and we assume that  $K_\sigma(x, dy)$  converges weakly to the delta measure in  $x$  as  $\sigma \downarrow 0$  while it converges to the base measure  $dy$  as  $\sigma \uparrow \infty$ .

**2.1 Heuristics: local moves versus global moves** Suppose that we want to modify  $K_\sigma(x, dy)$  and incorporate information about  $\pi$  in order to bias the proposal towards high-probability states. The first, somehow naive choice could be to consider the following localized version of  $\pi$

$$Q_\pi(x, dy) = \frac{\pi(y)K_\sigma(x, dy)}{Z_\sigma(x)}, \quad (1)$$

where  $Z_\sigma(x)$  is a normalizing constant. Assuming we could sample from it, we ask whether  $Q_\pi$  would be a good choice of proposal distribution. Equation (1) and the symmetry of  $K_\sigma$ ,  $K_\sigma(x, dy)dx = K_\sigma(y, dx)dy$ , implies that

$$\frac{Q_\pi(x, dy)dx}{\pi(y)Z_\sigma(y)} = \frac{Q_\pi(y, dx)dy}{\pi(x)Z_\sigma(x)},$$

which means that  $Q_\pi$  is reversible with respect to  $\pi(x)Z_\sigma(x)dx$ . Note that the normalizing constant  $Z_\sigma(x)$  is given by the convolution between  $\pi$  and  $K_\sigma$  which we denote by  $Z_\sigma(x) = (\pi * K_\sigma)(x) = \int_{\mathcal{X}} \pi(y)K_\sigma(x, dy)$ . Therefore, from the assumptions on  $K_\sigma$ , we have that  $Z_\sigma(x)$  converges to 1 for  $\sigma \uparrow \infty$ , while it converges to  $\pi(x)$  for  $\sigma \downarrow 0$ . It follows that the invariant measure of  $Q_\pi$  looks very different in the two opposite limiting regimes because

$$\pi(x)Z_\sigma(x) \rightarrow \begin{cases} \pi(x) & \text{if } \sigma \uparrow \infty \text{ (Global moves)} \\ \pi(x)^2 & \text{if } \sigma \downarrow 0 \text{ (Local moves)} \end{cases}.$$

Therefore, for big values of  $\sigma$ ,  $Q_\pi$  will be approximately  $\Pi$ -reversible and thus it would be a good proposal distribution for the Metropolis-Hastings algorithm. We thus refer to  $Q_\pi$  as *globally-balanced* proposal. On the contrary, for small values of  $\sigma$ ,  $Q_\pi$  would *not* be a good Metropolis-Hastings proposal because its invariant distribution converges to  $\pi(x)^2dx$  which is potentially very dissimilar from the target  $\pi(x)dx$ .

Following the previous arguments it is easy to correct for this behavior and design a proposal which is approximately  $\Pi$ -reversible for small values of  $\sigma$ . In particular one could consider replacing the biasing term  $\pi(y)$  in (1) with some transformation  $g(\pi(y))$ . A natural choice would be to consider  $\sqrt{\pi}$ , which leads to the proposal

$$Q_{\sqrt{\pi}}(x, dy) = \frac{\sqrt{\pi(y)} K_{\sigma}(x, dy)}{(\sqrt{\pi} * K_{\sigma})(x)}.$$

Arguing as before it is trivial to see that  $Q_{\sqrt{\pi}}$  is reversible with respect to  $\sqrt{\pi(x)}(\sqrt{\pi} * K_{\sigma})(x)dx$ , which converges to  $\pi(x)dx$  as  $\sigma \downarrow 0$ . We thus refer to  $Q_{\sqrt{\pi}}$  as an example of *locally-balanced proposal* with respect to  $\pi$ .

**2.2 Definition and characterization of locally-balanced proposals** In this work we will consider a specific class of informed proposal distributions, which we refer to as *pointwise informed* proposals. These proposals have the following structure

$$Q_{g,\sigma}(x, dy) = \frac{g\left(\frac{\pi(y)}{\pi(x)}\right) K_{\sigma}(x, dy)}{Z_g(x)} \quad (2)$$

where  $g$  is a continuous function from  $[0, \infty)$  to itself and  $Z_g(x)$  is the normalizing constant

$$Z_g(x) = \int_{\mathcal{X}} g\left(\frac{\pi(z)}{\pi(x)}\right) K_{\sigma}(x, dz). \quad (3)$$

The latter is finite by the continuity of  $g$  and boundedness of  $\pi$ . Throughout the paper, we assume  $g$  to be bounded by some linear function (i.e.  $g(t) \leq a + bt$  for some  $a$  and  $b$ ) to avoid integrability issues (see Appendix A.1).

The distribution  $Q_{g,\sigma}$  in (2) inherits the topological structure of  $K_{\sigma}$  and incorporates information regarding  $\Pi$  through the multiplicative term  $g\left(\frac{\pi(y)}{\pi(x)}\right)$ . Although the scheme in (2) is not the only way to design informed MH proposals, it is an interesting framework to consider. In particular it includes the uninformed choice  $Q(x, y) = K_{\sigma}(x, y)$  when  $g(t) = 1$ , and the “naively informed” choice  $Q(x, y) \propto K_{\sigma}(x, y)\pi(y)$  when  $g(t) = t$ . Given (2), the question of interest is how to choose the function  $g$ . In order to guide us in the choice of  $g$  we introduce the notion of locally-balanced kernels.

**Definition 1.** (*Locally-balanced kernels*) A family of Markov transition kernels  $\{Q_{\sigma}\}_{\sigma>0}$  is locally-balanced with respect to a distribution  $\Pi$  if each  $Q_{\sigma}$  is reversible with respect to some distribution  $\Pi_{\sigma}$  such that  $\Pi_{\sigma}$  converges weakly to  $\Pi$  as  $\sigma \downarrow 0$ .

The idea behind using a locally-balanced kernel  $Q_{\sigma}$  as a MH proposal targeting  $\Pi$  is that, in a local move regime (i.e. for small  $\sigma$ ),  $Q_{\sigma}$  will be almost  $\Pi$ -reversible and therefore the Metropolis-Hastings correction will have less job to do (namely correcting for the difference between  $\Pi_{\sigma}$  and  $\Pi$ ). This would allow for more moves to be accepted and longer moves to be performed, thus improving the algorithm’s efficiency. The reason to consider the local-move regime is that, as the dimensionality of the state space increases the MH moves typically become smaller and smaller with respect to the size of  $\mathcal{X}$ . These heuristic ideas will be confirmed by theoretical results and simulations studies in the following sections. The following theorem explicitly characterizes which pointwise informed proposal are locally-balanced.

**Theorem 1.** A pointwise informed proposal  $\{Q_{g,\sigma}\}_{\sigma>0}$  is locally-balanced with respect to a general  $\Pi$  if and only if

$$g(t) = t g(1/t) \quad \forall t > 0. \quad (4)$$

Motivated by Theorem 1 we refer to functions  $g$  satisfying (4) as balancing functions. In the next section we provide some results showing that locally-balanced proposals produce asymptotically more efficient MH algorithms compared to other pointwise informed proposals.

### 3 Peskun optimality of locally-balanced proposals

In this section we use Peskun ordering to compare the efficiency of Metropolis-Hastings (MH) schemes generated by pointwise informed proposals defined in (2). Unlike Section 2, where we considered the local limit  $\sigma \downarrow 0$ , we now consider a “fixed  $\sigma$ ” scenario, dropping the  $\sigma$  subscript and denoting the base kernel and corresponding pointwise informed proposals by  $K$  and  $Q_g$  respectively. We focus on discrete spaces, where Peskun-type results are more natural and broadly applicable. Thus we assume  $\mathcal{X}$  to be a finite space and  $dx$  to be the counting measure, meaning that  $\pi$  is the probability mass function of  $\Pi$  and  $K(x, y)$  is a symmetric transition matrix.

**3.1 Background on Peskun ordering** Peskun ordering provides a comparison result for Markov chains convergence properties. It measures the efficiency of MCMC algorithms in terms of *asymptotic variance* and *spectral gap*. The notion of asymptotic variance describes how the correlation among MCMC samples affects the variance of the empirical averages estimators. Given a  $\pi$ -stationary transition kernel  $P$  and a function  $h : \Omega \rightarrow \mathbb{R}$ , the asymptotic variance  $\text{var}_\pi(h, P)$  is defined as

$$\text{var}_\pi(h, P) = \lim_{T \rightarrow \infty} T \text{var} \left( \frac{\sum_{t=1}^T h(X_t)}{T} \right) = \lim_{T \rightarrow \infty} T^{-1} \text{var} \left( \sum_{t=1}^T h(X_t) \right),$$

where  $X_1, X_2, \dots$  is a Markov chain with transition kernel  $P$  started in stationarity (i.e. with  $X_1 \sim \pi$ ). The smaller  $\text{var}_\pi(h, P)$  the more efficient the corresponding MCMC algorithm is in estimating  $\mathbb{E}_\pi[h]$ . The spectral gap of a Markov transition kernel  $P$  is defined as  $\text{Gap}(P) = 1 - \lambda_2$ , where  $\lambda_2$  is the second largest eigenvalue of  $P$ , and always satisfy  $\text{Gap}(P) \geq 0$ . The value of  $\text{Gap}(P)$  is closely related to the convergence properties of  $P$ , with values close to 0 corresponding to slow convergence and values distant from 0 corresponding to fast convergence (see, e.g., [Levin et al., 2009, Ch.12-13] for a review of spectral theory for discrete Markov chains).

**Theorem 2.** *Let  $P_1$  and  $P_2$  be  $\pi$ -reversible Markov transition kernels on  $\mathcal{X}$  such that  $P_1(x, y) \geq c P_2(x, y)$  for all  $x \neq y$  and a fixed  $c > 0$ . Then it holds*

$$\begin{aligned} (a) \quad \text{var}_\pi(h, P_1) &\leq \frac{\text{var}_\pi(h, P_2)}{c} + \frac{1-c}{c} \text{var}_\pi(h) \quad \forall h : \mathcal{X} \rightarrow \mathbb{R}, \\ (b) \quad \text{Gap}(P_1) &\geq c \text{Gap}(P_2). \end{aligned}$$

The case  $c = 1$  of Theorem 2 is known as Peskun ordering [Peskun, 1973, Tierney, 1998]. Theorem 2 implies that if  $P_1(x, y) \geq c P_2(x, y)$  for all  $x \neq y$ , then  $P_1$  is “ $c$  times more efficient” than  $P_2$  in terms of spectral gap and asymptotic variances (ignoring the  $\text{var}_\pi(h)$  term which is typically much smaller than  $\text{var}_\pi(h, P_2)$  in non-trivial applications).

**3.2 Peskun comparison between pointwise informed proposals** In order to state Theorem 3 below, we define the following constant

$$c_g = \sup_{(x,y) \in \mathcal{R}} \frac{Z_g(y)}{Z_g(x)}, \quad (5)$$

where  $R = \{(x, y) \in \mathcal{X} \times \mathcal{X} : \pi(x)K(x, y) > 0\}$  and  $Z_g(x)$  is defined by (3).

**Theorem 3.** *Let  $g : (0, \infty) \rightarrow (0, \infty)$ . Define  $\tilde{g}(t) = \min\{g(t), t g(1/t)\}$  and let  $P_g$  and  $P_{\tilde{g}}$  be the MH kernels obtained from the pointwise informed proposals  $Q_g$  and  $Q_{\tilde{g}}$  defined as in (2). It holds*

$$P_{\tilde{g}}(x, y) \geq \frac{1}{c_g c_{\tilde{g}}} P_g(x, y) \quad \forall x \neq y. \quad (6)$$

The function  $\tilde{g}(t) = \min\{g(t), t g(1/t)\}$  satisfies  $\tilde{g}(t) = t \tilde{g}(1/t)$  by definition. Therefore Theorems 2 and 3 imply that for any  $g : \mathbb{R}_+ \rightarrow \mathbb{R}_+$  there is a corresponding balancing function  $\tilde{g}$  which leads to a more efficient MH algorithm modulo the factor  $\frac{1}{c_g c_{\tilde{g}}}$ . As we discuss in the next section, in many models of interest  $\frac{1}{c_g c_{\tilde{g}}}$  converges to 1 as the dimensionality of  $\mathcal{X}$  increases. When this is true we can deduce that locally-balanced proposals are asymptotically optimal in terms of Peskun ordering.

**3.3 High-dimensional regime** Suppose now that the distribution of interest  $\pi^{(n)}$  is indexed by a positive integer  $n$  which represents the dimensionality of the underlying state space  $\mathcal{X}^{(n)}$ . Similarly, also the base kernel  $K^{(n)}$  and the constants  $c_g^{(n)}$  defined by (5) depend on  $n$ . In many discrete contexts, as the dimensionality goes to infinity, the size of a single move of  $K^{(n)}$  becomes smaller and smaller with respect to the size of  $\mathcal{X}^{(n)}$  and does not change significantly the landscape around the current location. In those cases we would expect the following to hold

$$c_g^{(n)} \rightarrow 1 \quad \text{as } n \rightarrow \infty \quad (\text{A})$$

for every well-behaved  $g$  (e.g. bounded on compact subsets of  $(0, \infty)$ ). When (A) holds, the factor  $\frac{1}{c_g c_{\tilde{g}}}$  in the Peskun comparison of Theorem 3 converges to 1 and locally-balanced proposals are asymptotically optimal. For example, we expect the sufficient condition (A) to hold when the conditional independence graph of the model under consideration has a bounded degree and  $K^{(n)}$  updates a fixed number of variables at a time. We now describe three models involving discrete parameters which will be used as illustrative examples in the following sections and prove (A) for all of them.

**Example 1** (Independent binary components). *Consider  $\mathcal{X}^{(n)} = \{0, 1\}^n$  and, denoting the elements of  $\mathcal{X}^{(n)}$  as  $\mathbf{x}_{1:n} = (x_1, \dots, x_n)$ , the target distribution is*

$$\pi^{(n)}(\mathbf{x}_{1:n}) = \prod_{i=1}^n p_i^{1-x_i} (1-p_i)^{x_i},$$

where each  $p_i$  is a probability value in  $(0, 1)$ . The base kernel  $K^{(n)}(\mathbf{x}_{1:n}, \cdot)$  is the uniform distribution on the neighborhood  $N(\mathbf{x}_{1:n})$  defined as

$$N(\mathbf{x}_{1:n}) = \left\{ \mathbf{y}_{1:n} = (y_1, \dots, y_n) : \sum_{i=1}^n |x_i - y_i| = 1 \right\}.$$

**Example 2** (Weighted permutations). *Let*

$$\pi^{(n)}(\rho) = \frac{1}{Z} \prod_{i=1}^n w_{i\rho(i)} \quad \rho \in \mathcal{S}_n, \quad (7)$$

where  $\{w_{ij}\}_{i,j=1}^n$  are positive weights,  $Z$  is the normalizing constant  $\sum_{\rho \in \mathcal{S}_n} \prod_{i=1}^n w_{i\rho(i)}$  and  $\mathcal{S}_n$  is the space of permutations of  $n$  elements (i.e. bijections from  $\{1, \dots, n\}$  to itself).

We consider local moves that pick two indices and switch them. The induced neighboring structure is  $\{N(\rho)\}_{\rho \in \mathcal{S}_n}$  with

$$N(\rho) = \{\rho' \in \mathcal{S}_n : \rho' = \rho \circ (i, j) \text{ for some } i, j \in \{1, \dots, n\} \text{ with } i \neq j\}, \quad (8)$$

where  $\rho' = \rho \circ (i, j)$  is defined by  $\rho'(i) = \rho(j)$ ,  $\rho'(j) = \rho(i)$  and  $\rho'(l) = \rho(l)$  for  $l \neq i$  and  $l \neq j$ .

**Example 3** (Ising model). Consider the state space  $\mathcal{X}^{(n)} = \{-1, 1\}^{V_n}$ , where  $(V_n, E_n)$  is the  $n \times n$  square lattice graph with, for example, periodic boundary conditions. For each  $\mathbf{x} = (x_i)_{i \in V_n}$ , the target distribution is defined as

$$\pi^{(n)}(\mathbf{x}) = \frac{1}{Z} \exp \left( \sum_{i \in V_n} \alpha_i x_i + \lambda \sum_{(i, j) \in E_n} x_i x_j \right), \quad (9)$$

where  $\alpha_i \in \mathbb{R}$  are biasing terms representing the propensity of  $x_i$  to be positive,  $\lambda > 0$  is a global interaction term and  $Z$  is a normalizing constant. The neighbouring structure is the one given by single-bit flipping

$$N(\mathbf{x}) = \left\{ \mathbf{y} \in \mathcal{X}^{(n)} : \sum_{i \in V_n} |x_i - y_i| = 2 \right\}. \quad (10)$$

Example 1 is an illustrative toy example that we analyze explicitly in Section 4.2. Instead, the target measures in Examples 2 and 3 are non-trivial distributions to sample from that occur in many applied scenarios (see e.g. Sections 6 and 7), and MCMC schemes are among the most commonly used approaches to obtain approximate samples from those. Such examples will be used for illustrations in Sections 6.2 and 6.3. The following proposition, combined with Theorem 3, shows that for these examples locally-balanced proposal are asymptotically optimal within the class of pointwise informed proposals.

**Proposition 1.** *The following conditions are sufficient for Examples 1, 2 and 3 for (A) to hold for every locally bounded function  $g : (0, \infty) \rightarrow (0, \infty)$ :*

Example 1:  $\inf_{i \in \mathbb{N}} p_i > 0$ ,  $\sup_{i \in \mathbb{N}} p_i < 1$ ;

Example 2:  $\inf_{i, j \in \mathbb{N}} w_{ij} > 0$  and  $\sup_{i, j \in \mathbb{N}} w_{ij} < \infty$ ;

Example 3:  $\inf_{i \in \mathbb{N}} \alpha_i > -\infty$  and  $\sup_{i \in \mathbb{N}} \alpha_i < \infty$ .

## 4 Optimal choice of balancing function

In Section 3 we showed that, under the regularity assumption (A), locally-balanced proposals are asymptotically optimal in terms of Peskun ordering. It is thus natural to ask if there is an optimal proposal among the locally-balanced ones or, equivalently, if there is an optimal balancing function  $g$  among the ones satisfying  $g(t) = tg(1/t)$  (see Table 1). Before answering this question, we first draw a connection between the choice of balancing function  $g$  and the choice of acceptance probability function in the accept/reject step of the Metropolis-Hastings (MH) algorithm.

**4.1 Connection between balancing functions and acceptance probability functions.** The MH algorithm accepts each proposed state  $y$  with some probability  $a(x, y)$  which we refer to as acceptance probability function (APF). Denoting the ratio  $\frac{\pi(y)Q(y, x)}{\pi(x)Q(x, y)}$  by

	$g(t) = \sqrt{t}$	$g(t) = \frac{t}{1+t}$	$g(t) = 1 \wedge t$	$g(t) = 1 \vee t$
$Q_g(x, y) \propto$	$\sqrt{\pi(y)}K(x, y)$	$\frac{\pi(y)}{\pi(x)+\pi(y)}K(x, y)$	$\left(1 \wedge \frac{\pi(y)}{\pi(x)}\right)K(x, y)$	$\left(1 \vee \frac{\pi(y)}{\pi(x)}\right)K(x, y)$

Table 1: Examples of locally-balanced proposals  $Q_g$  obtained from different balancing functions  $g$ .

$t(x, y)$ , the Metropolis-Hastings APF can be written as  $a(x, y) = g(t(x, y))$  with  $g(t) = 1 \wedge t$ . It is well known that this is not the only possible choice: as long as

$$a(x, y) = t(x, y) a(y, x) \quad \forall x, y : Q(x, y) > 0, \quad (11)$$

the resulting kernel  $P$  is  $\pi$ -reversible and can be used for MCMC purposes. If we write  $a(x, y)$  as  $g(t(x, y))$ , condition (11) translates to

$$g(t) = tg(1/t).$$

The latter coincides with the condition for  $g$  to be a balancing function, see Theorem 1. Therefore each APF  $a(x, y) = g(t(x, y))$  corresponds to a balancing function  $g$ . However, the family of balancing functions is broader than the family of APFs because  $a(x, y) = g(t(x, y))$  are probabilities and thus need to be bounded by 1, while balancing functions don't. For example,  $g(t) = \sqrt{t}$  or  $1 \vee t$  are valid balancing functions but are not upper bounded by 1 and thus they are not a valid APF.

The connection with APFs is interesting because the latter are classical and well studied objects. In particular it is well-known that, in the context of APFs, the Metropolis-Hastings choice  $g(t) = 1 \wedge t$  is optimal and Peskun-dominates all other choices [Peskun, 1973, Tierney, 1998]. This fact, however, does not translate to the context of balancing functions. In the latter case the comparison between different  $g$ 's is more subtle and we expect no choice of balancing function to Peskun-dominate the others in general, not even asymptotically. In the next section we study a simple scenario and show that, in that case, the optimal balancing function is given by  $g(t) = \frac{t}{1+t}$ . Interestingly, the latter choice leads to a natural balancing term  $g(\frac{\pi(y)}{\pi(x)}) = \frac{\pi(y)}{\pi(x)+\pi(y)}$ , which has been previously considered in the context of APFs and is commonly referred to as Barker choice [Barker, 1965].

**4.2 The optimal proposal for independent binary variables** In this section we compare the efficiency of different locally-balanced proposals in the independent binary components case of Example 1. It turns out that in this specific case the Barker balancing function  $g(t) = \frac{t}{1+t}$  leads to the smallest mixing time.

From Example 1, each move from  $\mathbf{x}_{1:n}$  to a neighbouring state  $\mathbf{y}_{1:n} \in N(\mathbf{x}_{1:n})$  is obtained by flipping one component of  $\mathbf{x}_{1:n}$ , say the  $i$ -th bit, either from 0 to 1 or from 1 to 0. We denote the former by  $\mathbf{y}_{1:n} = \mathbf{x}_{1:n} + \mathbf{e}_{1:n}^{(i)}$  and the latter by  $\mathbf{y}_{1:n} = \mathbf{x}_{1:n} - \mathbf{e}_{1:n}^{(i)}$ . The pointwise informed proposal  $Q_g^{(n)}$  defined in (2) can then be written as

$$Q_g^{(n)}(\mathbf{x}_{1:n}, \mathbf{y}_{1:n}) = \frac{1}{Z_g^{(n)}(\mathbf{x}_{1:n})} \begin{cases} g(\frac{p_i}{1-p_i}) & \text{if } \mathbf{y}_{1:n} = \mathbf{x}_{1:n} + \mathbf{e}_{1:n}^{(i)}, \\ g(\frac{1-p_i}{p_i}) & \text{if } \mathbf{y}_{1:n} = \mathbf{x}_{1:n} - \mathbf{e}_{1:n}^{(i)}, \\ 0 & \text{if } \mathbf{y}_{1:n} \notin N(\mathbf{x}_{1:n}). \end{cases} \quad (12)$$

In order to compare the efficiency of  $Q_g^{(n)}$  for different choices of  $g$  we proceed in two steps. First we show that, after appropriate time-rescaling, the Metropolis-Hastings chain of interest converges to a tractable continuous time process as  $n \rightarrow \infty$  (Theorem 4). Secondly



we find which choice of  $g$  induces the fastest mixing on the limiting continuous-time process. Similar asymptotic approaches are well-established in the literature to compare MCMC schemes (see e.g. Roberts et al., 1997).

To simplify the following discussion we first rewrite  $Q_g^{(n)}$  as

$$Q_g^{(n)}(\mathbf{x}_{1:n}, \mathbf{y}_{1:n}) = \frac{1}{Z_g^{(n)}(\mathbf{x}_{1:n})} \begin{cases} v_i c_i (1 - p_i) & \text{if } \mathbf{y}_{1:n} = \mathbf{x}_{1:n} + \mathbf{e}_{1:n}^{(i)}, \\ v_i (1 - c_i) p_i & \text{if } \mathbf{y}_{1:n} = \mathbf{x}_{1:n} - \mathbf{e}_{1:n}^{(i)}, \\ 0 & \text{if } \mathbf{y}_{1:n} \notin N(\mathbf{x}_{1:n}), \end{cases} \quad (13)$$

where  $c_i \in (0, 1)$  and  $v_i > 0$  are the solution of  $v_i c_i (1 - p_i) = g(\frac{p_i}{1-p_i})$  and  $v_i (1 - c_i) p_i = g(\frac{p_i}{1-p_i})$ . Given (13), finding the optimal  $g$  corresponds to finding the optimal values for the two sequences  $(v_1, v_2, \dots)$  and  $(c_1, c_2, \dots)$ . In the following we assume  $\inf_{i \in \mathbb{N}} p_i > 0$ ,  $\sup_{i \in \mathbb{N}} p_i < 1$  and the existence of  $\lim_{n \rightarrow \infty} \frac{\sum_{i=1}^n v_i p_i (1-p_i)}{n} > 0$ . The latter is a mild assumption to avoid pathological behaviour of the sequence of  $p_i$ 's and guarantee the existence of a limiting process.

Let  $\mathbf{X}^{(n)}(t)$  be the MH Markov chain with proposal  $Q_g^{(n)}$  and target  $\pi^{(n)}$ . For any real time  $t$  and positive integer  $k \leq n$ , we define

$$S_{1:k}^{(n)}(t) = \left( X_1^{(n)}(\lfloor nt \rfloor), \dots, X_k^{(n)}(\lfloor nt \rfloor) \right),$$

with  $\lfloor nt \rfloor$  being the largest integer smaller than  $nt$ . Note that  $S_{1:k}^{(n)} = (S_{1:k}^{(n)}(t))_{t \geq 1}$  is a continuous-time (non-Markov) stochastic process on  $\{0, 1\}^k$  describing the first  $k$  components of  $(\mathbf{X}^{(n)}(t))_{t \geq 1}$ .

**Theorem 4.** *Let  $\mathbf{X}^{(n)}(1) \sim \pi^{(n)}$  for every  $n$ . For any positive integer  $k$ , it holds*

$$S_{1:k}^{(n)} \xrightarrow{n \rightarrow \infty} S_{1:k},$$

where  $\Rightarrow$  denotes weak convergence and  $S_{1:k}$  is a continuous-time Markov chain on  $\{0, 1\}^k$  with jumping rates given by

$$A(\mathbf{x}_{1:k}, \mathbf{y}_{1:k}) = \begin{cases} e_i(\mathbf{v}, c_i) \cdot (1 - p_i) & \text{if } \mathbf{y}_{1:k} = \mathbf{x}_{1:k} + \mathbf{e}_{1:k}^{(i)}, \\ e_i(\mathbf{v}, c_i) \cdot p_i & \text{if } \mathbf{y}_{1:k} = \mathbf{x}_{1:k} - \mathbf{e}_{1:k}^{(i)}, \\ 0 & \text{if } \mathbf{y}_{1:k} \notin N(\mathbf{x}_{1:k}) \text{ and } \mathbf{y}_{1:k} \neq \mathbf{x}_{1:k}, \end{cases} \quad (14)$$

where

$$e_i(\mathbf{v}, c_i) = \frac{1}{\bar{Z}(\mathbf{v})} v_i ((1 - c_i) \wedge c_i) \quad (15)$$

with  $\bar{Z}(\mathbf{v}) = \lim_{n \rightarrow \infty} \frac{\sum_{i=1}^n v_i p_i (1-p_i)}{n}$ .

We can now use Theorem 4 and the simple form of the limiting process  $S_{1:k}$  to establish what is the asymptotically optimal proposal  $Q_g^{(n)}$ . In fact (14) implies that, in the limiting process  $S_{1:k}$ , each bit is flipping independently of the others, with flipping rate of the  $i$ -th bit being proportional to  $e_i(\mathbf{v}, c_i)$ . Moreover, from (15) we see that the parameter  $c_i$  influences only the behaviour of the  $i$ -th component. Therefore, each  $c_i$  can be independently optimized by maximizing  $e_i(\mathbf{v}, c_i)$ , which leads to  $c_i = \frac{1}{2}$  for every  $i$ . By definition of  $c_i$ , the condition  $c_i = \frac{1}{2}$  corresponds to  $g(\frac{p_i}{1-p_i}) = \frac{p_i}{1-p_i} g(\frac{1-p_i}{p_i})$ . Therefore requiring  $c_i = \frac{1}{2}$  for all  $i$  corresponds to using a balancing function  $g$  satisfying  $g(t) = tg(1/t)$ . This is in accordance with the results of Section 3 and with the intuition that locally-balanced proposal are asymptotically optimal in high-dimensions.

Let us now consider the parameters  $(v_1, v_2, \dots)$ . Given  $c_i = \frac{1}{2}$ , different choices of  $(v_1, v_2, \dots)$  correspond to different locally-balanced proposals. From (15) we see that each  $v_i$  affects the flipping rate of all components through the normalizing constant  $\bar{Z}(\mathbf{v})$ , making the optimal choice of  $v_i$  less trivial. Intuitively, the parameter  $v_i$  represents how much effort we put into updating the  $i$ -th component, and increasing  $v_i$  reduces the effort put into updating other components. In order to discriminate among various choices of  $(v_1, v_2, \dots)$  we look for the choice that minimizes the mixing time of  $S_{1:k}$  for  $k$  going to infinity. Although this is not the only possible criterion to use, it is a reasonable and natural one. As we discuss in Appendix A.5.1, the latter is achieved by minimizing the mixing time of the slowest bit, which corresponds to choosing  $v_i$  constant over  $i$ . Intuitively, this means that we are sharing the sampling effort equally across components. It follows that the asymptotically optimal proposal  $Q_{g_{opt}}^{(n)}$  is

$$Q_{g_{opt}}^{(n)}(\mathbf{x}_{1:n}, \mathbf{y}_{1:n}) \propto \begin{cases} (1 - p_i) & \text{if } \mathbf{y}_{1:n} = \mathbf{x}_{1:n} + \mathbf{e}_{1:n}^{(i)}, \\ p_i & \text{if } \mathbf{y}_{1:n} = \mathbf{x}_{1:n} - \mathbf{e}_{1:n}^{(i)}, \\ 0 & \text{if } \mathbf{y}_{1:n} \notin N(\mathbf{x}_{1:n}). \end{cases} \quad (16)$$

The latter can be written as

$$Q_{g_{opt}}^{(n)}(\mathbf{x}_{1:n}, \mathbf{y}_{1:n}) \propto \frac{\pi^{(n)}(\mathbf{y}_{1:n})}{\pi^{(n)}(\mathbf{x}_{1:n}) + \pi^{(n)}(\mathbf{y}_{1:n})} \mathbb{1}_{N(\mathbf{x}_{1:n})}(\mathbf{y}_{1:n})$$

which means that the optimal balancing function is

$$g_{opt}(t) = \frac{t}{1+t}.$$

## 5 Connection to MALA and gradient-based MCMC

In the context of continuous state spaces, such as  $\mathcal{X} = \mathbb{R}^n$ , it is typically not feasible to sample efficiently from pointwise informed proposals as defined in (2). A natural thing to do in this context is to replace the intractable term in  $g(\frac{\pi(y)}{\pi(x)})$ , i.e. the target  $\pi(y)$ , with some local approximation around the current location  $x$ . For example, using a first-order Taylor expansion  $e^{\log \pi(y)} \approx e^{\log \pi(x) + \nabla \log \pi(x) \cdot (y-x)}$  we obtain a family of first-order informed proposals of the form

$$Q_{g,\sigma}^{(1)}(x, dy) \propto g\left(e^{\nabla \log \pi(x) \cdot (y-x)}\right) K_\sigma(x, dy), \quad (17)$$

for  $K_\sigma$  symmetric and  $g$  satisfying (4). Interestingly, the well known MALA proposal (e.g. Roberts and Rosenthal, 1998) can be obtained from (17) by choosing  $g(t) = \sqrt{t}$  and a gaussian kernel  $K_\sigma(x, \cdot) = N(x, \sigma^2)$ . Therefore we can think at MALA as a specific instance of locally-balanced proposal with first-order Taylor approximation. This simple and natural connection between locally-balanced proposals and classical gradient based schemes hints to many possible extensions of the latter, such as modifying the balancing function  $g$  or kernel  $K_\sigma$  or considering a different approximation for  $\pi(y)$ . The flexibility of the resulting framework could help to increase the robustness and efficiency of gradient-based methods. Recently, Titsias and Papaspiliopoulos [2016] considered different but related approaches to generalize gradient-based MCMC schemes, achieving state of the art sampling algorithms for various applications compared to both MALA and HMC. Given the focus of this paper on discrete spaces, we do not pursue this avenue here, leaving this research lines to future work (see Section 8).

## 6 Simulation studies

In this section we perform simulation studies using the target distributions of Examples 2 and 3. All computations are performed using the *R* programming language with code freely available upon request. The aim of the simulation study is two-folded: first comparing informed schemes with random walk ones, and secondly comparing different constructions of informed schemes among themselves.

**6.1 MCMC schemes under consideration** We compare six schemes: random walk MH (RW), a globally-balanced proposal (GB), two locally-balanced proposals (LB1 and LB2), the Hamming Ball sampler (HB) proposed in [Titsias and Yau, 2017] and the discrete HMC algorithm (D-HMC) proposed in Pakman and Paninski [2013]. The first four schemes (RW-GB-LB1-LB2) are Metropolis-Hastings algorithms with pointwise informed proposals of the form  $Q_g(x, y) \propto g\left(\frac{\pi(y)}{\pi(x)}\right) K(x, y)$ , with  $g(t)$  equal to 1,  $t$ ,  $\sqrt{t}$  and  $\frac{t}{1+t}$  respectively. HB is a data augmentation scheme that, given the current location  $x_t$ , first samples an auxiliary variable  $u \sim K(x_t, \cdot)$  and then samples the new state  $x_{t+1} \sim Q_\pi(u, \cdot)$ , where  $Q_\pi(u, y) \propto \pi(y)K(u, y)$  is defined as in (1). No acceptance-reject step is required as the chain is already  $\pi$ -reversible, being interpretable as a two stage Gibbs sampler on the extended state space  $(x, u)$  with target  $\pi(x)K(x, u)$ . To have a fair comparison, all these five schemes use the same base kernel  $K$ , defined as  $K(x, \cdot) = \text{Unif}(N(x))$  with neighbouring structures  $\{N(x)\}_{x \in \mathcal{X}}$  defined in Examples 2 and 3. Finally, D-HMC is a sampler specific to binary target distributions (thus applicable to Example 3 but not to Examples 2) constructed by first embedding the binary space in a continuous space and then applying HMC in the latter. For its implementation we followed Pakman and Paninski [2013], using a Gaussian distribution for the momentum variables and an integration time equal to  $2.5\pi$ . We will be talking about acceptance rates for all schemes, even if HB and D-HMC are not constructed as MH schemes. For HB, we define the acceptance rate as the proportion of times that the new state  $x_{t+1}$  is different from the previous state  $x_t$  (indeed the sampling procedure  $u \sim K(x_t, \cdot)$  and  $x_{t+1} \sim Q_\pi(u, \cdot)$  does often return  $x_{t+1} = x_t$ ). For D-HMC we define the acceptance rate as the proportion of times that a proposal to flip a binary component in the HMC flow is accepted (using the Pakman and Paninski [2013] terminology, the proportion of times that the particle crosses a potential wall rather than bouncing back). Such definitions will facilitate comparison with MH schemes.

**6.2 Sampling permutations** Consider the setting of Example 2, with target density  $\pi^{(n)}(\rho) \propto \prod_{i=1}^n w_{i\rho(i)}$  defined in (7) and base kernel  $K(\rho, \cdot)$  being the uniform distribution on the neighborhood  $N(\rho)$  defined in (8). The distribution  $\pi^{(n)}$  arises in many applied scenarios (e.g. Dellaert et al., 2003, Oh et al., 2009, Zanella, 2015) and sampling from the latter is a non-trivial task that is often accomplished with MCMC algorithms (see e.g. Jerrum and Sinclair [1996] for related complexity results).

For our simulations we first consider the case of i.i.d. weights  $\{w_{ij}\}_{i,j=1}^n$  with  $\log(w_{ij}) \sim N(0, \lambda^2)$ . Here  $n$  and  $\lambda$  provide control on the dimensionality and the smoothness of the target distribution respectively. For example, when  $\lambda = 0$  the target distribution is uniform and the five schemes under consideration (D-HMC not applicable) collapse to the same transition kernel, which is  $K(\rho, \cdot)$  itself (modulo HB performing two steps per iteration). On the other hand, as  $\lambda$  increases the difference between RW and informed schemes becomes more prominent (Figure 1). In fact, for “rough” distributions, most states proposed by RW have small probability under the target and get rejected. Despite being more robust than RW, also GB and HB suffer from high rejection rates as  $\lambda$  increase. On the

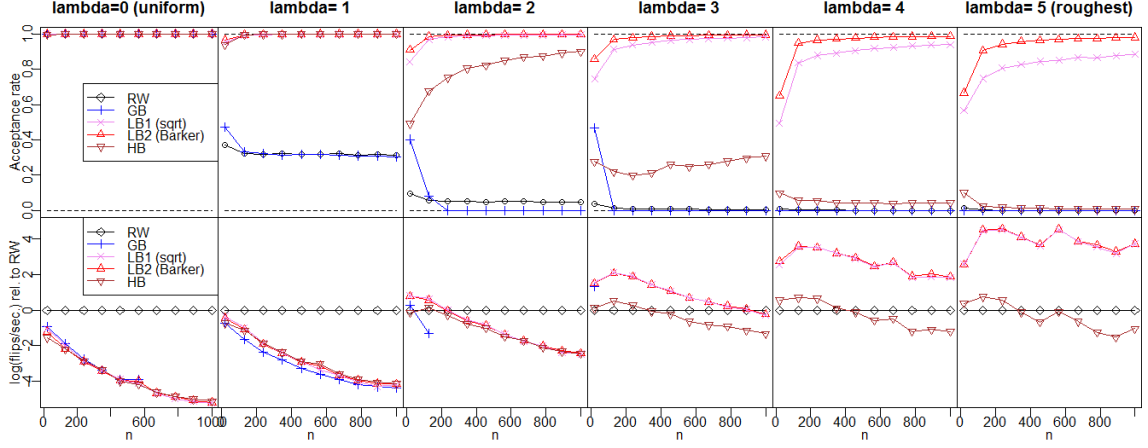


Figure 1: Behaviour of the five MCMC schemes under consideration when targeting Example 2 with  $\log(w_{ij}) \stackrel{iid}{\sim} N(0, \lambda^2)$  for varying  $n$  and  $\lambda$ . First row: average acceptance rates. Second row: number of flips per unit of computation time relative to RW (on log scale).

contrary, the acceptance rates of LB1 and LB2, which are designed to be asymptotically  $\pi$ -reversible, approaches 1 as  $n$  increases for all values of  $\lambda$  considered (Figure 1, first row). In order to take into account the cost per iteration, which is substantially higher for informed schemes, we then compare the number of successful “flips” (i.e. switches of two indices) per unit of computation time. The latter is a useful and easy to estimate diagnostic that provides a first gross indication of the relative efficiency of the various schemes. Figure 1 suggests that for flatter targets (i.e. small values of  $\lambda$ ) the computational overhead required to use informed proposal schemes is not worth the effort, as a plain RW proposal achieves the highest number of flips per unit time. However, as the roughness increases and the target distribution becomes more challenging to explore, informed proposals (in particular LB1 and LB2) achieve a much higher number of flips per unit time. Similar conclusions are obtained by using more advanced diagnostic tools, such as effective sample size per unit time. For example, Figure 2 displays the results for  $n = 500$  and  $\lambda = 5$ , suggesting that for rough targets locally-balanced schemes are one to two orders of magnitude more efficient than the other schemes under consideration (see Supplement B.1 for results for all values of  $\lambda$ ). Note that GB is extremely sensitive to the starting state: if the latter

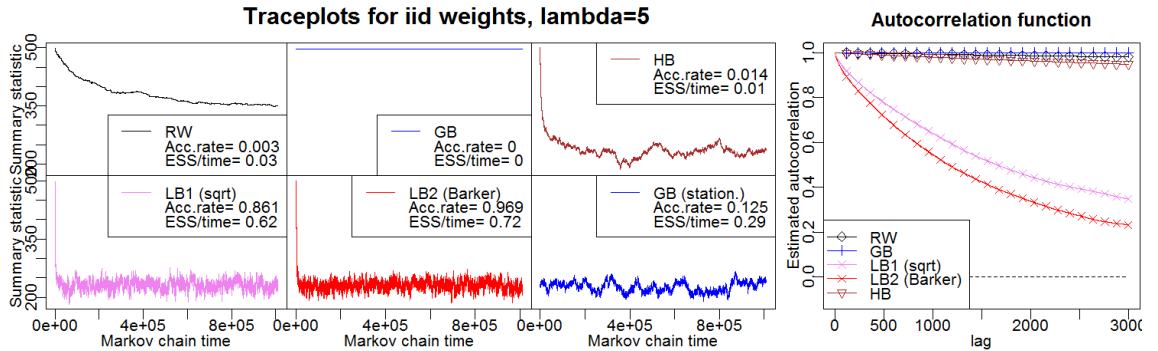


Figure 2: Setting:  $n = 500$  and  $\log(w_{ij}) \stackrel{iid}{\sim} N(0, \lambda^2)$  with  $\lambda = 5$ . Left: traceplots of a summary statistic (Hamming distance from fixed permutation). Right: estimated autocorrelation functions.

is unlikely under the target (e.g. a uniformly at random permutation) the chain gets stuck and reject almost all moves, while if started in stationarity (i.e. from a permutation approx. drawn from the target) the chain has a more stable behaviour (see Figure 2).

Finally, consider a more structured case where, rather than iid weights, we sample  $w_{ij} \sim \exp(-\chi_{|i-j|}^2)$ . The resulting matrix  $\{w_{ij}\}_{i,j=1}^n$  has a banded-like structure, with

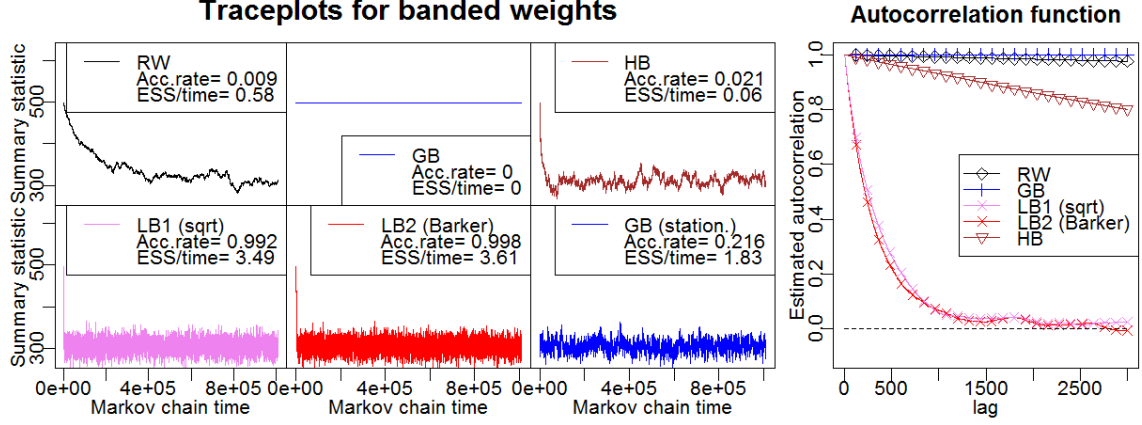


Figure 3: Setting:  $n = 500$  and  $w_{ij} \sim \exp(-\chi_{|i-j|}^2)$ . Left: traceplots of a summary statistic (Hamming distance from fixed permutation). Right: estimated autocorrelation functions.

weights getting smaller with distance from the diagonal. Figure 3 shows the performances of the different schemes. The results are similar to the iid case, with an even more prominent difference in efficiency between HB and LB1-LB2.

**6.3 Ising model** Consider now the Ising model described in Example 3. The latter is a classic model used in many scientific areas, e.g. statistical mechanics and spatial statistics. In this simulation study we consider target distributions motivated by Bayesian image analysis, where one seeks to partition an image into objects and background. In the simplest version of the problem, each pixel  $i$  needs to be classified as object ( $x_i = 1$ ) or background ( $x_i = -1$ ). One approach to such task is to define a Bayesian model, using the Ising model (or the Potts model in more general multi-objects contexts) as a prior distribution to induce positive correlation among neighboring pixels. The resulting posterior distribution is made of a prior term  $\exp(\lambda \sum_{(i,j) \in E_n} x_i x_j)$  times a likelihood term  $\exp(\sum_{i \in V_n} \alpha_i x_i)$ , which combined produce a distribution of the form (9). See Supplement B.2 for more details on the derivation of such distributions and Moores et al. [2015a] for recent applications to computed tomography.

Similarly to Section 6.2, we considered an array of target distributions, varying the size of the  $n \times n$  grid and the concentration of the target distribution (controlled by the strength of spatial correlation  $\lambda$  and signal-to-noise ratio in the likelihood terms  $\alpha_i$ ). Figure 4 reports the acceptance rates and number of flips per unit of computing time for the six MCMC schemes under consideration and for five levels of target concentration (see Supplement B.2 for full details on the set up for  $\lambda$  and the  $\alpha_i$ 's). RW, GB and D-HMC have very low acceptance rates for all non-uniform distributions considered (see the Appendix of Pakman and Paninski [2013] for discussion on the similar acceptance rates between RW and D-HMC). HB, LB1 and LB2 on the contrary do not suffer from high rejection rates and achieve a much higher number of flips per unit time. However, despite having a good number of flips per second, HB suffers from poor mixing in most cases considered (see e.g. Figure 5 and Supplement B.2 for more examples). In summary, the results are similar to

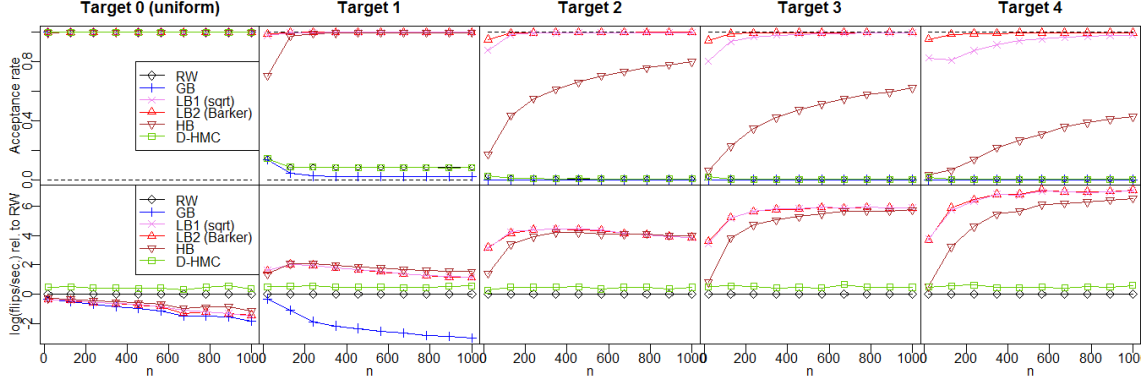


Figure 4: Behaviour of the six MCMC schemes under consideration when targeting Example 3 for varying  $n$  and level of concentration of the target. First row: average acceptance rates. Second row: number of flips per unit of computing time relative to RW (on log scale).

Section 6.2, with locally balanced schemes (LB1 and LB2) being orders of magnitude more efficient than alternative schemes especially when targeting highly non-uniform targets (see effective sample sizes per unit time in Figure 5 and Supplement B.2).

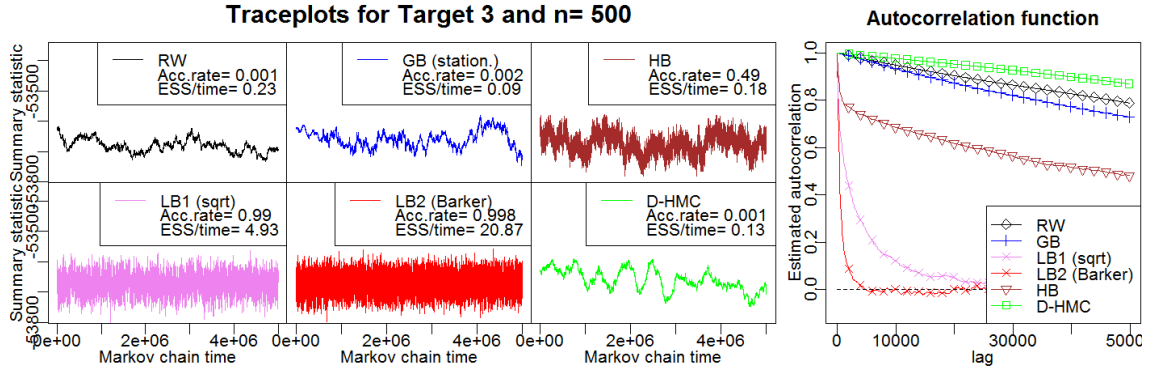


Figure 5: Setting: Ising model with  $n = 500$ ,  $\lambda = 1$  and  $\alpha_i$ 's described in Supplement B.2. Left: traceplots of a summary statistic (Hamming distance from fixed permutation). For D-HMC the plot displays the whole trajectory, including the path during the integration period. Right: estimated autocorrelation functions.

Given the focus of this work, we do not considered specialized algorithms for the Ising model performing global updates (e.g. Swendsen and Wang [1987]). The latter are somehow complementary to the single-site updating schemes considered here as they perform much better when the target is multimodal (e.g. in the absence of informative likelihood terms and with moderately strong interaction term  $\lambda$ ), while they perform poorly in cases where the likelihood terms  $\{\alpha_i\}_{i \in V_n}$  dominate, like the image analysis context considered here (see e.g. Hurn [1997] and Moores et al. [2015b] for more discussion).

**6.4 Block-wise implementation** In many scenarios, as the dimensionality of the state space increases, also the computational cost of sampling from the pointwise informed proposals as defined in (2) increases. For example, in discrete space settings it is typical to have a base kernel  $K(x, \cdot)$  which is a uniform distribution on some neighborhood  $N(x) \subseteq \mathcal{X}$  whose size grows with the dimensionality of  $\mathcal{X}$ . In these cases, when the size

of  $N(x)$  becomes too large, it may be inefficient to use an informed proposal on the whole neighborhood  $N(x)$ . Rather, it may be more efficient to first select a sub-neighborhood  $N'(x) \subseteq N(x)$  at random, and then apply locally-balanced proposals to the selected sub-space. For example, if the state space under consideration has a Cartesian product structure, then one could update a subset of variables given the others in a *block-wise* fashion, analogously to the Gibbs Sampling context. By choosing appropriately the size of  $N'(x)$  one can obtain an appropriate trade-off between computational cost (a small  $N'(x)$  induces an informed proposal that is cheap to sample) and statistical efficiency (a large  $N'(x)$  produces better informed moves as it considers more candidate states at each step). Such an approach is illustrated in Section 7 and Supplement C.4 on a record linkage application. See also Titsias and Yau [2017] for additional discussion on block-wise implementations and the resulting cost-vs-efficiency tradeoff in the context of the Hamming Ball sampler and Section 8 for related comments in future works discussion.

## 7 Application to Bayesian record linkage

Record linkage, also known as entity resolution, is the process of identifying which records refer to the same entity across two or more databases with potentially repeated entries. Such operation is typically performed to remove duplicates when merging different databases. If records are potentially noisy and unique identifiers are not available, statistical methods are needed to perform reliable record linkage operations. While traditional record linkage methodologies are based on the early work Fellegi and Sunter [1969], Bayesian approaches to record linkage are receiving increasing attention in recent years [Tancredi et al., 2011, Steorts et al., 2016, Sadinle, 2017, Johndrow et al., 2017]. Such approaches are particularly interesting, for example, as they provide uncertainty statements on the linkage procedure that can be naturally propagated to subsequent inferences, such as population-size estimation [Tancredi et al., 2011]. Despite recent advances in Bayesian modeling for record linkage problems (see e.g. Zanella et al. [2016]), exploring the posterior distribution over the space of possible linkage configurations is still a computationally challenging task which is limiting the applicability of Bayesian record linkage methodologies. In this section we use locally-balanced proposals to derive efficient samplers for Bayesian record linkage.

We consider bipartite record linkage tasks, where one seeks to merge two databases with duplicates occurring across databases but not within. This is the most commonly considered case in the record linkage literature (see Sadinle [2017] and references therein). Denote by  $\mathbf{x} = (x_1, \dots, x_{n_1})$  and  $\mathbf{y} = (y_1, \dots, y_{n_2})$  the two databases under consideration. In this context, the parameter of interest is a partial matching between  $\{1, \dots, n_1\}$  and  $\{1, \dots, n_2\}$ , where  $i$  is matched with  $j$  if and only if  $x_i$  and  $y_j$  represent the same entity. We represent such a matching with a  $n_1$ -dimensional vector  $\mathbf{M} = (M_1, \dots, M_{n_1})$ , where  $M_i = j$  if  $x_i$  is matched with  $y_j$  and  $M_i = 0$  if  $x_i$  is not matched with any  $y_j$ . In Supplement C we specify a Bayesian model for bipartite record linkage, assuming the number of entities and the number of duplicates to follow Poisson distributions a priori, and assuming the joint distribution of  $(\mathbf{x}, \mathbf{y})$  given  $\mathbf{M}$  to follow a spike-and-slab categorical distribution (often called hit-miss model in the Record Linkage literature [Copas and Hilton, 1990]). The unknown parameters of the model are the partial matching  $\mathbf{M}$  and two real-valued hyperparameters  $\lambda$  and  $p_{match}$ , representing the expected number of entities and the probability of having a duplicate for each entity. We perform inferences in a Metropolis-within-Gibbs fashion, where we alternate sampling  $(p_{match}, \lambda) | \mathbf{M}$  and  $\mathbf{M} | (p_{match}, \lambda)$ , see Supplement C.3 for full details on the sampler. While it is straightforward to sample from the two-dimensional distribution  $(p_{match}, \lambda) | \mathbf{M}$ , see (42)-(43) in Supplement C for explicit

full conditionals, providing an efficient way to update the high-dimensional discrete object  $\mathbf{M}$  is more challenging and this is where we exploit locally-balanced proposals.

We consider a dataset derived from the Italian Survey on Household and Wealth, which is a biennial survey conducted by the Bank of Italy. The dataset is publicly available (e.g. through the *Italy* R package) and consists of two databases, the 2008 survey (covering 13,702 individuals) and the 2010 one (covering 13,733 individuals). For each individual, the survey recorded 11 variables, such as year of birth, sex and working status.

First, following Steorts [2015], we perform record linkage for each Italian region separately. This results in 20 separate record linkage tasks with roughly 1300 individuals each on average. We ran four MCMC schemes for each record linkage task and compare their performances. Following the notation of Section 6, the four schemes are RW, GB, LB and HB, where LB refers to the locally-balanced proposals with Barker weights. Figure 6(a) shows the number of matches over MCMC iterations for region 1 (other regions show a similar qualitative behaviour). We can see that LB and HB converge rapidly to the region of substantial posterior probability, while RW and GB exhibit an extremely slow convergence. HB, however, converges and mixes significantly slower than LB (see e.g. the autocorrelation functions in 6(b)). To provide a quantitative comparison between the per-

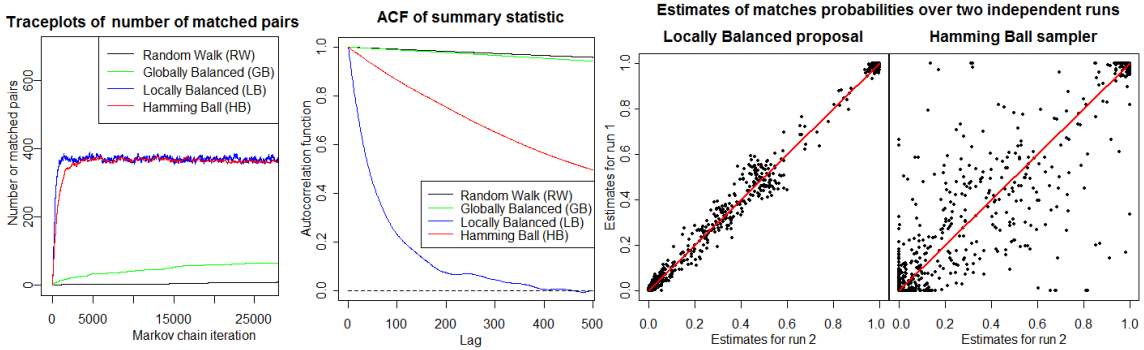


Figure 6: Output analysis for the 4 MCMC schemes under comparison applied to the Italy dataset (region 1).

formances of the four schemes, we consider as efficiency measure the effective sample sizes per unit of computation time relative to RW. Effective sample sizes are computed using the coda R package [Plummer et al., 2006] and averaged over 5 summary statistics (each summary statistics being the Hamming distance from a matching randomly drawn from the posterior). From Table 2 we can see that LB provides roughly two orders of magnitude improvement in efficiency over RW and GB and one order of magnitude improvement over HB. Indeed from Figure 6(c) we can see that, given the same computational budget, LB

Region	1	2	3	4	5	6	7	8	Average
GB vs RW	0.8	2.9	0.7	1.7	1.4	0.5	1.0	0.9	0.94
LB vs RW	60.6	209	36.2	127	48.9	104	172	33.3	94.0
HB vs RW	6.3	20.3	3.7	15.3	7.2	10.9	15.6	3.1	9.96

Table 2: Relative efficiency (defined as ESS/time) of GB, LB and HB compared to RW . The table reports the value for the first 8 regions and the average over all 20 regions.

manages to provide much more reliable estimates of the posterior probabilities of each couple being matched compared to HB. Computations were performed using the *R* programming language. For each region we ran LB for 35000 iterations (enough to produce



reliable estimates of posterior pairwise matching probabilities like the one in Figure 6(c)), requiring on average around 120 seconds per region.

Next, we consider the task of performing recording linkage on the whole Italy dataset, without dividing it first into regions. In fact the latter operation (typically referred to as deterministic blocking in the record linkage literature) is typically done for computational reasons but has the drawback of excluding a priori possible matches across groups (in this case regions). We apply LB to the whole dataset using the block-wise implementation discussed in Section 6.4 (details in Supplement C.4). Standard output analysis suggests that the LB chain is converging fast (Figure 7, left) and mixing well in the region of substantial probability (Figure 7, center). Comparing independent runs of the algorithms

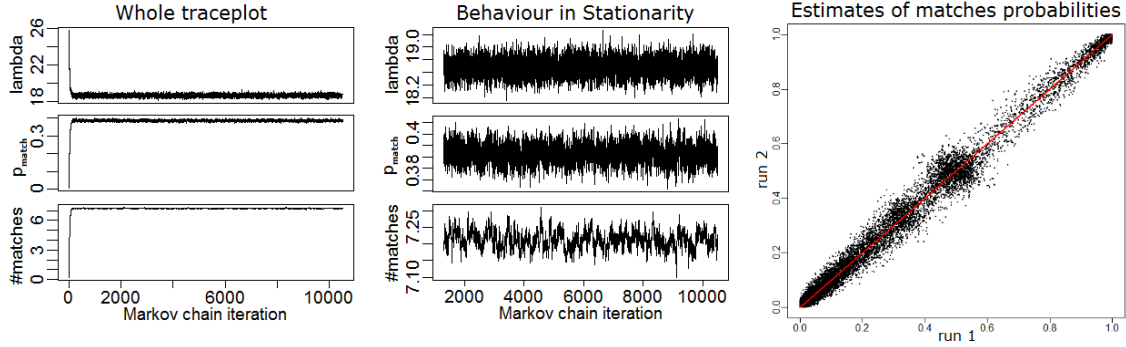


Figure 7: Output analysis for locally-balanced MCMC applied to the full Italy dataset (see Section 7).

suggests that we are obtaining reliable estimates of the nearly one billion posterior pairwise matching probabilities (Figure 7, right). The simulation needed to obtain the probability estimates in Figure 7(right) took less than 40 minutes with a plain *R* implementation on a single desktop computer.

## 8 Discussion and future work

In this work we discussed a fundamental and yet not satisfactorily answered question in the MCMC methodology literature, which is how to design “informed” Metropolis-Hastings proposals in discrete spaces. We proposed a simple and original framework (pointwise informed proposals and locally-balanced criteria) that provides useful and easy-to-implement methodological guidance. Under regularity assumptions, we were able to prove the optimality of locally-balanced proposals in high-dimensional regimes and to identify the optimal elements within such class. The theoretical results of Sections 2-4 are confirmed by simulations (Sections 6-7), where we observe orders of magnitude improvements in efficiency over alternative schemes both for simulated and real data scenarios. We envisage that locally-balanced proposals could be helpful in various contexts to be incorporated as a building block in more elaborate Monte Carlo algorithms. The proposed methodology can be applied to arbitrary statistical models with discrete-valued parameters, such as Bayesian Nonparametric models or model selection problems.

The present work offers many directions for possible extentions and future work. For example, the connection to MALA in Section 5 could be exploited to improve the robustness of gradient-based MCMC schemes and reduce the notoriously heavy burden associated with their tuning procedures. Also, it would be interesting to extend our study to the popular context of Multiple-Try Metropolis (MTM) schemes [Liu et al., 2000]. In fact, the MTM weight function, used to select the proposed point among candidate ones, plays a role that

is very similar to one of multiplicative biasing terms in pointwise informed proposals and we expect our results to translate quite naturally to that context.

In terms of implementation, it would be interesting to explore in more depth the trade-off between computational cost per iteration and statistical efficiency of the resulting Markov chain. Beyond the use of block-wise implementations discussed in Section 6.4, another approach to reduce the cost per iteration would be to replace the informed term  $g(\frac{\pi(y)}{\pi(x)})$  in the proposal with some cheap-to-evaluate approximation, while still using the exact target in the MH accept/reject step. Also, the computations required to sample from locally-balanced proposals are trivially parallelizable and specific hardware for parallel computations, such as Graphics Processing Units (GPUs), could be used to reduce the computational overhead required by using informed proposals [Lee et al., 2010].

From the theoretical point of view, it would be interesting to provide guidance for a regime which is intermediate between local and global, maybe by designing appropriate interpolations between locally-balanced and globally-balanced proposals. This could be useful to design schemes that adaptively learn the appropriate level of interpolation needed. Also, one could prove the sufficient condition for optimality (A) in much more general contexts. Finally, throughout the paper we assumed the base kernel  $K_\sigma$  to be symmetric and it would be interesting to extend the results to the case of general base kernels.

**Acknowledgements** The author is grateful to Gareth Roberts, Omiros Papaspiliopoulos and Samuel Livingstone for useful suggestions and stimulating discussions. This work was supported in part by an EPSRC Doctoral Prize fellowship and by the European Research Council (ERC) through StG “N-BNP” 306406.

## References

- A. A. Barker. Monte carlo calculations of the radial distribution functions for a proton-electron plasma. *Australian Journal of Physics*, 18(2):119–134, 1965.
- J. Barrera, B. Lachaud, and B. Ycart. Cut-off for n-tuples of exponentially converging processes. *Stochastic processes and their applications*, 116(10):1433–1446, 2006.
- J. Bon and E. Păltănea. Convergence of the number of failed components in a Markov system with nonidentical components. *Journal of applied probability*, 38(4):882–897, 2001.
- J. Copas and F. Hilton. Record linkage: statistical models for matching computer records. *Journal of the Royal Statistical Society. Series A (Statistics in Society)*, pages 287–320, 1990.
- F. Dellaert, S. Seitz, C. Thorpe, and S. Thrun. EM, MCMC, and chain flipping for structure from motion with unknown correspondence. *Machine Learning*, 50(1-2):45–71, 2003.
- P. Diaconis and L. Saloff-Coste. Logarithmic Sobolev inequalities for finite Markov chains. *The Annals of Applied Probability*, 6(3):695–750, 1996.
- A. Durmus, G. O. Roberts, G. Vilmart, K. C. Zygalakis, et al. Fast langevin based algorithm for mcmc in high dimensions. *The Annals of Applied Probability*, 27(4):2195–2237, 2017.
- S. Ethier and T. Kurtz. Markov processes: Characterization and convergence. 1986.
- I. P. Fellegi and A. B. Sunter. A theory for record linkage. *Journal of the American Statistical Association*, 64(328):1183–1210, 1969.

- M. Girolami and B. Calderhead. Riemann manifold Langevin and Hamiltonian monte carlo methods. *Journal of the Royal Statistical Society: Series B (Statistical Methodology)*, 73(2):123–214, 2011.
- W. K. Hastings. Monte Carlo sampling methods using Markov chains and their applications. *Biometrika*, 57(1):97–109, 1970.
- M. Hurn. Difficulties in the use of auxiliary variables in Markov chain Monte Carlo methods. *Statistics and Computing*, 7(1):35–44, 1997.
- M. Jerrum and A. Sinclair. The Markov chain Monte Carlo method: an approach to approximate counting and integration. *Approximation algorithms for NP-hard problems*, pages 482–520, 1996.
- J. E. Johndrow, K. Lum, and D. B. Dunson. Theoretical Limits of Record Linkage and Microclustering. *arXiv preprint arXiv:1703.04955*, 2017.
- K. Łatuszyński and G. O. Roberts. CLTs and asymptotic variance of time-sampled Markov chains. *Methodology and Computing in Applied Probability*, pages 1–11, 2013.
- A. Lee, C. Yau, M. B. Giles, A. Doucet, and C. C. Holmes. On the utility of graphics cards to perform massively parallel simulation of advanced Monte Carlo methods. *Journal of computational and graphical statistics*, 19(4):769–789, 2010.
- D. Levin, Y. Peres, and E. Wilmer. *Markov chains and mixing times*. American Mathematical Soc., 2009.
- J. S. Liu, F. Liang, and W. H. Wong. The multiple-try method and local optimization in metropolis sampling. *Journal of the American Statistical Association*, 95(449):121–134, 2000.
- N. Metropolis, A. W. Rosenbluth, M. N. Rosenbluth, A. H. Teller, and E. Teller. Equation of state calculations by fast computing machines. *The journal of chemical physics*, 21(6):1087–1092, 1953.
- J. Miller, B. Betancourt, A. Zaidi, H. Wallach, and R. C. Steorts. Microclustering: When the cluster sizes grow sublinearly with the size of the data set. *arXiv preprint arXiv:1512.00792*, 2015.
- A. Mira. Ordering and improving the performance of Monte Carlo Markov chains. *Statistical Science*, pages 340–350, 2001.
- M. T. Moores, C. E. Hargrave, T. Deegan, M. Poulsen, F. Harden, and K. Mengersen. An external field prior for the hidden Potts model with application to cone-beam computed tomography. *Computational Statistics & Data Analysis*, 86:27–41, 2015a.
- M. T. Moores, A. N. Pettitt, and K. Mengersen. Scalable Bayesian inference for the inverse temperature of a hidden Potts model. *arXiv preprint arXiv:1503.08066*, 2015b.
- R. Neal. MCMC using Hamiltonian dynamics. In S. Brooks, A. Gelman, G. Jones, and X. Meng, editors, *Handbook of Markov Chain Monte Carlo*. CRC press, 2011.
- A. Nishimura, D. Dunson, and J. Lu. Discontinuous Hamiltonian Monte Carlo for sampling discrete parameters. *arXiv preprint arXiv:1705.08510*, 2017.
- S. Oh, S. Russell, and S. Sastry. Markov chain Monte Carlo data association for multi-target tracking. *Automatic Control, IEEE Transactions on*, 54(3):481–497, 2009.
- A. Pakman and L. Paninski. Auxiliary-variable exact Hamiltonian Monte Carlo samplers for binary distributions. In *Advances in neural information processing systems*, pages 2490–2498, 2013.

- P. Peskun. Optimum monte-carlo sampling using Markov chains. *Biometrika*, 60(3):607–612, 1973.
- M. Plummer, N. Best, K. Cowles, and K. Vines. Coda: Convergence diagnosis and output analysis for mcmc. *R News*, 6(1):7–11, 2006. URL <https://journal.r-project.org/archive/>.
- C. Robert and G. Casella. Monte Carlo Statistical Methods. 2005.
- G. Roberts and J. Rosenthal. Optimal scaling of discrete approximations to Langevin diffusions. *Journal of the Royal Statistical Society. Series B, Statistical Methodology*, pages 255–268, 1998.
- G. Roberts, A. Gelman, and W. Gilks. Weak convergence and optimal scaling of random walk Metropolis algorithms. *The Annals of Applied Probability*, 7(1):110–120, 1997.
- M. Sadinle. Bayesian estimation of bipartite matchings for record linkage. *Journal of the American Statistical Association*, pages 1–13, 2017.
- R. C. Steorts. Entity resolution with empirically motivated priors. *Bayesian Analysis*, 10(4):849–875, 2015.
- R. C. Steorts, R. Hall, and S. E. Fienberg. A bayesian approach to graphical record linkage and deduplication. *Journal of the American Statistical Association*, 111(516):1660–1672, 2016.
- R. H. Swendsen and J.-S. Wang. Nonuniversal critical dynamics in Monte Carlo simulations. *Physical review letters*, 58(2):86, 1987.
- A. Tancredi, B. Liseo, et al. A hierarchical Bayesian approach to record linkage and population size problems. *The Annals of Applied Statistics*, 5(2B):1553–1585, 2011.
- L. Tierney. A note on Metropolis-Hastings kernels for general state spaces. *Annals of Applied Probability*, pages 1–9, 1998.
- M. K. Titsias and O. Papaspiliopoulos. Auxiliary gradient-based sampling algorithms. *arXiv preprint arXiv:1610.09641*, 2016.
- M. K. Titsias and C. Yau. The hamming ball sampler. *Journal of the American Statistical Association*, pages 1–14, 2017.
- M. Welling and Y. Teh. Bayesian learning via stochastic gradient Langevin dynamics. In *Proceedings of the 28th International Conference on Machine Learning (ICML-11)*, pages 681–688, 2011.
- G. Zanella. Random partition models and complementary clustering of Anglo-Saxon place-names. *The Annals of Applied Statistics*, 9(4):1792–1822, 2015.
- G. Zanella, B. Betancourt, J. W. Miller, H. Wallach, A. Zaidi, and R. C. Steorts. Flexible models for microclustering with application to entity resolution. In *Advances in Neural Information Processing Systems*, pages 1417–1425, 2016.
- Y. Zhang, Z. Ghahramani, A. J. Storkey, and C. A. Sutton. Continuous Relaxations for Discrete Hamiltonian Monte Carlo. In *Advances in Neural Information Processing Systems*, pages 3194–3202, 2012.

## A Additional calculations and proofs

**A.1 Proof of Theorem 1** To prove Theorem 1 we first need a technical Lemma to show that a linear bound on  $g$  is sufficient to ensure that the integral  $\int_{\mathcal{X}} \pi(x) Z_{g,\sigma}(x) dx$  is well behaved.

**Lemma 1.** *Let  $g : [0, \infty) \rightarrow [0, \infty)$  with  $g(1) = 1$  and  $g(t) \leq a + bt$  for some  $a, b \geq 0$  and all  $t \geq 0$ . Given a bounded density function  $\pi : \mathcal{X} \rightarrow (0, \infty)$ , a family of symmetric kernels  $K_\sigma(x, dy)$  such that  $K_\sigma(x, dy) \Rightarrow \delta_x(dy)$  for all  $x \in \mathcal{X}$  as  $\sigma \downarrow 0$  and  $Z_{g,\sigma}(x)$  defined as in (3), it holds*

$$\lim_{\sigma \rightarrow 0} \int_{\mathcal{X}} \pi(x) Z_{g,\sigma}(x) dx = 1.$$

*Proof of Lemma 1.* For every  $x \in \mathcal{X}$  it holds  $Z_{g,\sigma}(x) \pi(x) \rightarrow \pi(x)$  as  $\sigma \downarrow 0$ , see e.g. (23). Therefore, Fatou's Lemma guarantees

$$\liminf_{\sigma \rightarrow 0} \int_{\mathcal{X}} \pi(x) Z_{g,\sigma}(x) dx \geq \int_{\mathcal{X}} \pi(x) dx = 1. \quad (18)$$

We now show that the corresponding limsup is upper bounded by 1. To do so, fix  $\epsilon > 0$  and let  $A$  be an open subset of  $\mathcal{X}$  such that  $\int_A dx < \infty$  and  $\Pi(A) > 1 - \epsilon$ . Using the Bounded Convergence Theorem it can be easily seen that

$$\lim_{\sigma \rightarrow 0} \int_A \pi(x) Z_{g,\sigma}(x) dx = \int_A \pi(x) dx = \Pi(A). \quad (19)$$

In fact  $\int_A dx < \infty$  by assumption and  $\pi(x) Z_{g,\sigma}(x)$  is bounded over  $x$  because

$$\begin{aligned} \pi(x) \int_{\mathcal{X}} g\left(\frac{\pi(y)}{\pi(x)}\right) K_\sigma(x, dy) &\leq \pi(x) \int_{\mathcal{X}} \left(a + b \frac{\pi(y)}{\pi(x)}\right) K_\sigma(x, dy) = \\ &= a\pi(x) + b \int_{\mathcal{X}} \pi(y) K_\sigma(x, dy) \leq (a + b) \sup_{z \in \mathcal{X}} \pi(z). \end{aligned}$$

Consider then the integral over  $A^c$ . From  $g(t) \leq a + bt$  we have

$$\begin{aligned} \int_{A^c} \pi(x) Z_{g,\sigma}(x) dx &\leq \int_{A^c} \pi(x) \int_{\mathcal{X}} \left(a + b \frac{\pi(y)}{\pi(x)}\right) K_\sigma(x, dy) dx = \\ &= a\Pi(A^c) + b \int_{x \in A^c, y \in \mathcal{X}} \pi(y) K_\sigma(x, dy) dx. \end{aligned} \quad (20)$$

Using the reversibility of  $K_\sigma$  w.r.t.  $dx$  we can bound the latter integral as follows

$$\begin{aligned} \int_{x \in A^c, y \in \mathcal{X}} \pi(y) K_\sigma(x, dy) dx &= \int_{y \in \mathcal{X}} \pi(y) \int_{x \in A^c} K_\sigma(y, dx) dy = \\ &= \int_{y \in \mathcal{X}} \pi(y) K_\sigma(y, A^c) dy \leq \Pi(A^c) + \int_{y \in A} \pi(y) K_\sigma(y, A^c) dy. \end{aligned} \quad (21)$$

The term  $K_\sigma(y, A^c)$  is upper bounded by 1 and converges to 0 for every  $y \in A$  because  $A^c$  is a closed set and  $K_\sigma(y, \cdot) \Rightarrow \delta_y(\cdot)$  as  $\sigma \downarrow 0$ . Therefore by the Bounded Convergence Theorem  $\int_{y \in A} \pi(y) K_\sigma(y, A^c) dy \rightarrow 0$  as  $\sigma \downarrow 0$ . Combining (19), (20) and (21) we obtain

$$\limsup_{\sigma \rightarrow 0} \int_{\mathcal{X}} \pi(x) Z_{g,\sigma}(x) dx \leq \Pi(A) + a\Pi(A^c) + b\Pi(A^c) \leq 1 + (a + b)\epsilon.$$

From the arbitrariness of  $\epsilon$  it follows  $\limsup_{\sigma \rightarrow 0} \int_{\mathcal{X}} \pi(x) Z_{g,\sigma}(x) dx = 1$  as desired.  $\square$

*Proof of Theorem 1. Sufficiency.* Suppose that (4) holds and, without loss of generality,  $g(1) = 1$ . Using the definition of  $Q_{g,\sigma}$  and the symmetry of  $K_\sigma$  it holds

$$\frac{Z_{g,\sigma}(x)Q_{g,\sigma}(x, dy)dx}{g\left(\frac{\pi(y)}{\pi(x)}\right)} = K_\sigma(x, dy)dx = K_\sigma(y, dx)dy = \frac{Z_{g,\sigma}(y)Q_{g,\sigma}(y, dx)dy}{g\left(\frac{\pi(x)}{\pi(y)}\right)}. \quad (22)$$

From (4) it follows  $g\left(\frac{\pi(x)}{\pi(y)}\right) = \frac{\pi(x)}{\pi(y)}g\left(\frac{\pi(y)}{\pi(x)}\right)$ . The latter, together with (22) implies

$$\pi(x)Z_{g,\sigma}(x)Q_{g,\sigma}(x, dy)dx = \pi(y)Z_{g,\sigma}(y)Q_{g,\sigma}(y, dx)dy.$$

Therefore  $Q_{g,\sigma}$  is reversible w.r.t.  $\frac{\pi(x)Z_{g,\sigma}(x)dx}{\int_{\mathcal{X}} \pi(z)Z_{g,\sigma}(z)dz}$ , where  $\int_{\mathcal{X}} \pi(z)Z_{g,\sigma}(z)dz$  is finite by Lemma 1. Since  $K_\sigma(x, \cdot) \Rightarrow \delta_x(\cdot)$  by assumption (see Section 2) and since  $z \rightarrow g\left(\frac{\pi(z)}{\pi(x)}\right)$  is a bounded and continuous function, it follows that

$$Z_{g,\sigma}(x) = \int_{\mathcal{X}} g\left(\frac{\pi(z)}{\pi(x)}\right) K_\sigma(x, dz) \xrightarrow{\sigma \downarrow 0} \int_{\mathcal{X}} g\left(\frac{\pi(z)}{\pi(x)}\right) \delta_x(dz) = g(1), \quad (23)$$

for every  $x \in \mathcal{X}$ . Combining (23) and Lemma 1 we deduce that the probability density function  $\frac{\pi(x)Z_{g,\sigma}(x)}{\int_{\mathcal{X}} \pi(z)Z_{g,\sigma}(z)dz}$  converges pointwise to  $\pi(x)$  for every  $x \in \mathcal{X}$ . It follows by Scheffé's Lemma that  $\frac{\pi(x)Z_{g,\sigma}(x)dx}{\int_{\mathcal{X}} \pi(z)Z_{g,\sigma}(z)dz}$  converges weakly to  $\pi(x)dx$ .

*Necessity.* Suppose (4) does not hold and therefore  $g(t_0) \neq t_0 g(\frac{1}{t_0})$  for some  $t_0 > 0$ . To prove that (4) is a necessary condition for  $\{Q_{g,\sigma}\}_{\sigma>0}$  to be locally-balanced with respect to a general  $\Pi(dx) = \pi(x)dx$  with bounded and continuous density  $\pi$ , it is enough to provide a counterexample. Consider then  $\mathcal{X} = \{0, 1\}$ ,  $dx$  being the counting measure,  $\pi(0) = \frac{1}{1+t_0}$  and  $\pi(1) = \frac{t_0}{1+t_0}$ . From (22) it follows that  $Q_{g,\sigma}$  is reversible with respect to  $\Pi_\sigma(dx) = \pi_\sigma(x)dx$ , where  $\pi_\sigma = (\pi_\sigma(1), \pi_\sigma(2))$  is proportional to  $(\frac{\pi(0)Z_{g,\sigma}(0)}{g(t_0)}, \frac{\pi(1)Z_{g,\sigma}(1)}{t_0 g(\frac{1}{t_0})})$ . From  $K_\sigma(x, \cdot) \Rightarrow \delta_x(\cdot)$  it follows that  $\Pi_\sigma(dx) \Rightarrow \Pi_0(dx) = \pi_0(x)dx$  with  $\pi_0 = (\pi_0(1), \pi_0(2))$  proportional to  $(\frac{\pi(0)}{g(t_0)}, \frac{\pi(1)}{t_0 g(\frac{1}{t_0})})$ . Finally,  $g(t_0) \neq t_0 g(\frac{1}{t_0})$  implies that  $\Pi_0 \neq \Pi$  and thus  $\Pi_\sigma \not\Rightarrow \Pi$ .  $\square$

**A.2 Proof of Theorem 2** To prove part (a) of Theorem 2 we need the following Lemma (see also Łatuszyński and Roberts [2013, Corollary 1] for a similar result in the context of general state spaces  $\mathcal{X}$ ).

**Lemma 2.** *Let  $P$  be a  $\Pi$ -reversible Markov transition kernels on a finite space  $\mathcal{X}$ . Let  $\tilde{P} = cP + (1-c)Id$ , where  $Id$  is the identity kernel and  $c \in (0, 1]$ . Then it holds*

$$\text{var}_\pi(h, \tilde{P}) = \frac{\text{var}_\pi(h, P)}{c} + \frac{1-c}{c} \text{var}_\pi(h) \quad \forall h \in L^2(\Pi).$$

*Proof of Lemma 2.* Suppose  $\mathbb{E}_\pi[h] = 0$  (otherwise consider  $h - \mathbb{E}_\pi[h]$ ). Also, if  $P$  is reducible then the statement is trivially true, so suppose  $P$  to be irreducible. Let  $\{(\lambda_i, f_i)\}_{i=1}^n$  and  $\{(\tilde{\lambda}_i, \tilde{f}_i)\}_{i=1}^n$  be eigenvalues and eigenfunctions of  $P$  and  $\tilde{P}$  respectively. We can take  $\{f_i\}_{i=1}^n$  and  $\{\tilde{f}_i\}_{i=1}^n$  to be an orthonormal basis of  $L^2(\mathbb{R}^{\mathcal{X}}, \pi)$  with  $\lambda_1 = \tilde{\lambda}_1 = 1$ ,  $f_1 = \tilde{f}_1 = (1, \dots, 1)^T$  and  $-1 \leq \lambda_i, \tilde{\lambda}_i < 1$  for  $i \geq 2$  [Levin et al., 2009, Lemmas 12.1, 12.2]. Also, from the definition of  $\tilde{P}$ , it follows that we can take  $\tilde{f}_i = f_i$  and  $\tilde{\lambda}_i = c\lambda_i + (1-c)$ . The asymptotic variances can be written as

$$\text{var}_\pi(h, P) = \sum_{i=2}^n \frac{1+\lambda_i}{1-\lambda_i} \mathbb{E}_\pi[h f_i]^2 \quad \text{and} \quad \text{var}_\pi(h, \tilde{P}) = \sum_{i=2}^n \frac{1+\tilde{\lambda}_i}{1-\tilde{\lambda}_i} \mathbb{E}_\pi[h \tilde{f}_i]^2. \quad (24)$$

For (24) see for example the proofs of Mira [2001, Theorem 1] and Levin et al. [2009, Lemmas 12.20]. Rearranging  $\tilde{\lambda}_i = c\lambda_i + (1-c)$  we obtain  $\frac{1+\tilde{\lambda}_i}{1-\tilde{\lambda}_i} = \frac{1}{c}\frac{1+\lambda_i}{1-\lambda_i} + \frac{1-c}{c}$  for  $i \geq 2$ . Thus

$$\text{var}_\pi(h, \tilde{P}) = \sum_{i=2}^n \frac{1+\tilde{\lambda}_i}{1-\tilde{\lambda}_i} \mathbb{E}_\pi[h f_i]^2 = \frac{1}{c} \sum_{i=2}^n \frac{1+\lambda_i}{1-\lambda_i} \mathbb{E}_\pi[h f_i]^2 + \frac{1-c}{c} \sum_{i=2}^n \mathbb{E}_\pi[h f_i]^2. \quad (25)$$

Since  $\{f_i\}_{i=1}^n$  form an orthonormal basis of  $L^2(\mathbb{R}^{\mathcal{X}}, \pi)$  and  $\mathbb{E}_\pi[h f_1] = \mathbb{E}_\pi[h] = 0$ , then  $\sum_{i=2}^n \mathbb{E}_\pi[h f_i]^2 = \mathbb{E}_\pi[h^2] = \text{var}_\pi(h)$ . Therefore (25) becomes  $\text{var}_\pi(h, \tilde{P}_1) = \frac{1}{c} \cdot \text{var}_\pi(h, P_1) + \frac{1-c}{c} \text{var}_\pi(h)$ .  $\square$

*Proof of Theorem 2.* Part (a), case  $c > 1$ : define  $\tilde{P}_1 = \frac{1}{c}P_1 + (1 - \frac{1}{c})\mathbb{I}_n$ . From Lemma 2 it follows  $\text{var}_\pi(h, \tilde{P}_1) = c \cdot \text{var}_\pi(h, P_1) + (c-1) \text{var}_\pi(h)$  or, equivalently,  $\text{var}_\pi(h, P_1) = \frac{1}{c} \text{var}_\pi(h, \tilde{P}_1) + \frac{1-c}{c} \text{var}_\pi(h)$ . Since  $\tilde{P}_1(x, y) \geq P_2(x, y)$  for  $x \neq y$ , by Theorem Peskun [1973, Thm.2.1.1] it holds  $\text{var}_\pi(h, \tilde{P}_1) \leq \text{var}_\pi(h, P_2)$ . Therefore

$$\text{var}_\pi(h, P_1) = \frac{\text{var}_\pi(h, \tilde{P}_1)}{c} + \frac{1-c}{c} \text{var}_\pi(h) \leq \frac{\text{var}_\pi(h, P_2)}{c} + \frac{1-c}{c} \text{var}_\pi(h).$$

Part (a), case  $c \leq 1$ : define  $\tilde{P}_2 = cP_2 + (1-c)\mathbb{I}_n$ . From Peskun [1973, Thm.2.1.1] and  $P_1(x, y) \geq \tilde{P}_2(x, y)$  for  $x \neq y$  it follows  $\text{var}_\pi(h, P_1) \leq \text{var}_\pi(h, \tilde{P}_2)$ . From Lemma 2 it follows  $\text{var}_\pi(h, \tilde{P}_2) = \frac{1}{c} \text{var}_\pi(h, P_2) + \frac{1-c}{c} \text{var}_\pi(h)$ . The latter equality and  $\text{var}_\pi(h, P_1) \leq \text{var}_\pi(h, \tilde{P}_2)$  provide us with part (a).

Part (b) follows from the definition of  $\text{Gap}(P)$ .  $\square$

**A.3 Proof of Theorem 3** In this section we state and prove a slightly more general result than Theorem 3, namely Theorem 5. The latter applies also to continuous spaces and include both upper and lower bounds. Theorem 3 is kept in the main body of the paper for simplicity of exposition.

As in the beginning of Section 2, let  $\Pi(dx) = \pi(x)dx$  be a target probability distribution on some topological space  $\mathcal{X}$  with bounded density  $\pi$  with respect to some reference measure  $dx$  and let  $K(x, dy)$  be a symmetric Markov kernel on  $\mathcal{X}$ . Define  $R \subseteq \mathcal{X} \times \mathcal{X}$  as the set where the two measures  $\Pi(dx)K(x, dy)$  and  $\Pi(dy)K(y, dx)$  are mutually absolutely continuous (Tierney [1998, Prop.1] shows that  $R$  is unique up to sets of zero mass for both measures) and for any  $(x, y)$  in  $R$  denote by  $t_{xy}$  the Radon-Nikodym derivative  $\frac{\Pi(dy)K(y, dx)}{\Pi(dx)K(x, dy)}$ . Note that  $R$  is also the set where  $\Pi(dx)Q_g(x, dy)$  and  $\Pi(dy)Q_g(y, dx)$  are mutually absolutely continuous. Define

$$b_g = \sup_{(x, y) \in R} \frac{g(t_{xy})}{t_{xy}g(t_{yx})} \geq 1, \quad (26)$$

and

$$c_g = \sup_{(x, y) \in R} \frac{Z_g(y)}{Z_g(x)} \geq 1. \quad (27)$$

The suprema in (26) and (27) have to be intended  $\Pi(dx)K(x, dy)$ -almost everywhere. Both  $b_g$  and  $c_g$  are greater or equal than one because, by inverting  $x$  and  $y$  both the fraction in (26) and (27) get inverted. The constant  $b_g$  represents how “unbalanced” the function  $g$  is: the bigger  $b_g$  the less balanced  $g$  is according to (4) (if  $b_g = 1$  then  $g$  satisfies (4)). It is easy to see that the following result implies Theorem 3 as a special case.

**Theorem 5.** Let  $g : (0, \infty) \rightarrow (0, \infty)$ . Define  $\tilde{g}(t) = \min\{g(t), t g(1/t)\}$  and let  $P_g$  and  $P_{\tilde{g}}$  be the MH kernels obtained from the proposals  $Q_g$  and  $Q_{\tilde{g}}$  respectively (see (2) for definition). For  $\Pi$ -almost every  $x$  it holds

$$\frac{P_{\tilde{g}}(x, A)}{c_g c_{\tilde{g}} b_g} \leq P_g(x, A) \leq (c_g c_{\tilde{g}}) P_{\tilde{g}}(x, A) \quad \forall A \not\ni x. \quad (28)$$

*Proof of theorem 5.* Let  $x \notin A \subseteq \mathcal{X}$ . By construction,  $P_g(x, \cdot)$  is absolutely continuous with respect to  $K(x, \cdot)$  on  $\mathcal{X} \setminus \{x\}$ . In particular, given  $y \in \mathbb{R}$  with  $y \neq x$ , the Radon-Nikodym derivative between  $P_g(x, \cdot)$  and  $K(x, \cdot)$  at  $y$  satisfies

$$\frac{P_g(x, dy)}{K(x, dy)} = \frac{g(t_{xy})}{Z_g(x)} \min \left\{ 1, t_{xy} \frac{g(t_{yx})}{Z_g(y)} \frac{Z_g(x)}{g(t_{xy})} \right\} = \min \left\{ \frac{g(t_{xy})}{Z_g(x)}, \frac{t_{xy} g(t_{yx})}{Z_g(y)} \right\}. \quad (29)$$

Using (29) and the definition of  $c_g$ , it follows that for  $\Pi$ -almost every  $x$

$$\frac{1}{c_g} \frac{\min \{g(t_{xy}), t_{xy} g(t_{yx})\}}{Z_g(x)} \leq \frac{P_g(x, dy)}{K(x, dy)} \leq c_g \frac{\min \{g(t_{xy}), t_{xy} g(t_{yx})\}}{Z_g(x)}. \quad (30)$$

Using (30), the definition of  $\tilde{g}$  and the inequality  $Z_g(x) \geq Z_{\tilde{g}}(x)$  (which follows from  $g(t) \geq \tilde{g}(t)$ ) we can deduce that for  $\Pi$ -almost every  $x$

$$P_g(x, A) \leq c_g \int_A \frac{\tilde{g}(t_{xy})}{Z_g(x)} K(x, dy) \leq c_g \int_A \frac{\tilde{g}(t_{xy})}{Z_{\tilde{g}}(x)} K(x, dy), \quad (31)$$

Using the analogous of (30) for  $\tilde{g}$  rather than  $g$ , we have

$$P_{\tilde{g}}(x, A) \geq \frac{1}{c_{\tilde{g}}} \int_A \frac{\min \{\tilde{g}(t_{xy}), t_{xy} \tilde{g}(t_{yx})\}}{Z_{\tilde{g}}(x)} K(x, dy) = \frac{1}{c_{\tilde{g}}} \int_A \frac{\tilde{g}(t_{xy})}{Z_{\tilde{g}}(x)} K(x, dy). \quad (32)$$

The upper bound in (28) follows from (31) and (32). To obtain the lower bound in (28) first note that using the lower bound in (30) and the definition of  $b_g$  for  $\Pi$ -almost every  $x$  it holds

$$P_g(x, A) \geq \frac{1}{c_g} \int_A \frac{\min \{g(t_{xy}), t_{xy} g(t_{yx})\}}{Z_g(x)} K(x, dy) \geq \frac{1}{b_g c_g} \int_A \frac{g(t_{xy})}{Z_g(x)} K(x, dy). \quad (33)$$

Then note that

$$P_{\tilde{g}}(x, A) = \int_A \min \left\{ \frac{\tilde{g}(t_{xy})}{Z_{\tilde{g}}(x)}, \frac{t_{xy} \tilde{g}(t_{yx})}{Z_{\tilde{g}}(y)} \right\} K(x, dy) \leq \frac{1}{c_{\tilde{g}}} \int_A \frac{\tilde{g}(t_{xy})}{Z_{\tilde{g}}(x)} K(x, dy). \quad (34)$$

□

#### A.4 Proof of Proposition 1

*Proof of Proposition 1.* Consider Example 2. Fix  $\rho \in \mathcal{S}_n$  and  $\rho' = \rho \circ (i_0, j_0)$  for some  $i_0, j_0 \in \{1, \dots, n\}$ , with  $i_0 < j_0$ . Denoting  $g\left(\frac{\pi^{(n)}(\rho \circ (i, j))}{\pi^{(n)}(\rho)}\right) = g\left(\frac{w_{i\rho(j)} w_{j\rho(i)}}{w_{i\rho(i)} w_{j\rho(j)}}\right)$  by  $g_{ij}^\rho$  it holds

$$Z_g^{(n)}(\rho) = \sum_{i,j=1, i < j}^n g_{ij}^\rho = \sum_{\substack{i,j=1, i < j \\ \{i,j\} \cap \{i_0, j_0\} = \emptyset}}^n g_{ij}^\rho + \sum_{\substack{i,j=1, i < j \\ \{i,j\} \cap \{i_0, j_0\} \neq \emptyset}}^n g_{ij}^\rho.$$



Given  $I = \left[ \frac{\inf_{i,j} w_{ij}^2}{\sup_{i,j} w_{ij}^2}, \frac{\sup_{i,j} w_{ij}^2}{\inf_{i,j} w_{ij}^2} \right]$ ,  $\underline{g} = \inf_{t \in I} g(t)$  and  $\bar{g} = \sup_{t \in I} g(t)$  it holds  $\underline{g} \leq g_{ij}^\rho \leq \bar{g}$ . Note that  $\underline{g} > 0$  and  $\bar{g} < \infty$  because  $g$  and  $1/g$  are locally bounded and  $I$  is compact. Therefore

$$\sum_{\substack{i,j=1, i < j \\ \{i,j\} \cap \{i_0, j_0\} = \emptyset}}^n g_{ij}^\rho \geq \sum_{\substack{i,j=1, i < j \\ \{i,j\} \cap \{i_0, j_0\} = \emptyset}}^n \underline{g} = \left( \frac{n(n-1)}{2} - (2n-3) \right) \underline{g} = O(n^2)$$

and

$$\sum_{\substack{i,j=1, i < j \\ \{i,j\} \cap \{i_0, j_0\} \neq \emptyset}}^n g_{ij}^\rho \leq \sum_{\substack{i,j=1, i < j \\ \{i,j\} \cap \{i_0, j_0\} \neq \emptyset}}^n \bar{g} = (2n-3)\bar{g} = O(n).$$

It follows that

$$\lim_{n \rightarrow \infty} \frac{Z_g^{(n)}(\rho')}{Z_g^{(n)}(\rho)} = \lim_{n \rightarrow \infty} \frac{\sum_{\{i,j\} \cap \{i_0, j_0\} = \emptyset} g_{ij}^\rho}{\sum_{\{i,j\} \cap \{i_0, j_0\} = \emptyset} g_{ij}^{\rho'}} = \lim_{n \rightarrow \infty} \frac{\sum_{\{i,j\} \cap \{i_0, j_0\} = \emptyset} g_{ij}^\rho}{\sum_{\{i,j\} \cap \{i_0, j_0\} = \emptyset} g_{ij}^\rho} = 1,$$

where  $g_{ij}^\rho = g_{ij}^{\rho'}$  for  $\{i,j\} \cap \{i_0, j_0\} = \emptyset$  because  $\rho'(i) = \rho(i)$  for  $i \in \{1, \dots, n\} \setminus \{i_0, j_0\}$ .

The proofs for Example 1 and 3 are analogous.  $\square$

**A.5 Proof of Theorem 4** To prove Theorem 4 we first need the following Lemma.

**Lemma 3.** *For every positive integers  $k < n$ , let*

$$R_n^{(k)} = \left\{ (x_{k+1}, \dots, x_n) \in \{0, 1\}^{n-k} : \left| \frac{Z_g^{(n)}(\mathbf{x}_{1:n})}{n} - \mathbb{E} \left[ \frac{Z_g^{(n)}(\mathbf{X}_{1:n})}{n} \right] \right| \leq \frac{1}{n^{1/4}} \quad \forall (x_1, \dots, x_k) \in \Omega^{(k)} \right\}. \quad (35)$$

Then it holds  $\lim_{n \rightarrow \infty} \pi^{(n)}(\{0, 1\}^k \times R_n^{(k)}) = 1$ .

*Proof of Lemma 3.* From (13) it follows

$$Z_g^{(n)}(\mathbf{x}_{1:n}) = \sum_{i=1}^n v_i (c_i(1-p_i)(1-x_i) + (1-c_i)p_i x_i).$$

Thus, for  $\mathbf{X}_{1:n} \sim \pi^{(n)}$ , it holds  $\mathbb{E} \left[ \frac{Z_g^{(n)}(\mathbf{X}_{1:n})}{n} \right] = \sum_{i=1}^n v_i p_i (1-p_i)$ . Using the triangular inequality we can split

$$\left| \frac{Z_g^{(n)}(\mathbf{x}_{1:n})}{n} - \mathbb{E} \left[ \frac{Z_g^{(n)}(\mathbf{X}_{1:n})}{n} \right] \right| \leq \frac{\left| \sum_{i=1}^k m_i \right|}{n} + \frac{\left| \sum_{i=k+1}^n m_i \right|}{n}, \quad (36)$$

where  $m_i = v_i (c_i(1-p_i)(1-x_i) + (1-c_i)p_i x_i - p_i(1-p_i))$ . Note that each  $m_i$  is upper bounded by  $2 \sup_{i \in \mathbb{N}} v_i$  because  $p_i, x_i$  and  $c_i$  belong to  $[0, 1]$ , while the finiteness of  $\sup_{i \in \mathbb{N}} v_i$  can be deduced by the definition of  $v_i$ 's and the assumptions  $\sup_{i \in \mathbb{N}} p_i < 1$  and  $\inf_{i \in \mathbb{N}} p_i > 0$ .

Therefore  $\frac{\left| \sum_{i=1}^k m_i \right|}{n} \leq \frac{2k \sup_{i \in \mathbb{N}} v_i}{n}$  which will eventually be smaller than  $\frac{1}{2n^{1/4}}$  as  $n$  increases.

Consider now last sum in (36),  $\frac{\left| \sum_{i=k+1}^n m_i \right|}{n}$ , which depends on  $\mathbf{x}_{1:n}$  only through the  $x_i$ 's with  $i > k$ . For  $\mathbf{X}_{1:n} \sim \pi^{(n)}$  and  $M_i = v_i (c_i(1-p_i)(1-X_i) + (1-c_i)p_i X_i - p_i(1-p_i))$ , the random variable  $\frac{\sum_{i=k+1}^n M_i}{n}$  has mean zero and variance upper bounded by  $\frac{\sup_{i \in \mathbb{N}} v_i^2}{n-k}$ .

Therefore, using for example the Markov inequality, we have  $P\left(\frac{\left| \sum_{i=k+1}^n M_i \right|}{n} \geq \frac{1}{2n^{1/4}}\right) \rightarrow 0$  as  $n$  increases. It follows the thesis.  $\square$

*Proof of Theorem 4.* Let  $k$  be fixed and denote by  $A^{(n)}(\mathbf{x}_{1:k}, \mathbf{y}_{1:k})$  the jumping rates of  $S_{1:k}^{(n)}$  from  $\mathbf{x}_{1:k}$  to  $\mathbf{y}_{1:k}$ . By construction, for any  $\mathbf{y}_{1:k} \neq \mathbf{x}_{1:k}$  and  $\mathbf{y}_{1:k} \notin N(\mathbf{x}_{1:k})$ , it holds  $A^{(n)}(\mathbf{x}_{1:k}, \mathbf{y}_{1:k}) = 0$ . Also, it is easy to see that, if  $x_i = 0$ , it holds

$$A^{(n)}(\mathbf{x}_{1:k}, \mathbf{x}_{1:k} + \mathbf{e}_{1:k}^{(i)}) = \frac{v_i(1-p_i)}{\frac{Z_g^{(n)}(\mathbf{x}_{1:n})}{n}} \left( c_i \wedge \left( (1-c_i) \frac{Z_g^{(n)}(\mathbf{x}_{1:n})}{Z_g^{(n)}(\mathbf{x}_{1:n} + \mathbf{e}_{1:n}^{(i)})} \right) \right),$$

while if  $x_i = 1$

$$A^{(n)}(\mathbf{x}_{1:k}, \mathbf{x}_{1:k} - \mathbf{e}_{1:k}^{(i)}) = \frac{v_i p_i}{\frac{Z_g^{(n)}(\mathbf{x}_{1:n})}{n}} \left( (1-c_i) \wedge \left( c_i \frac{Z_g^{(n)}(\mathbf{x}_{1:n})}{Z_g^{(n)}(\mathbf{x}_{1:n} - \mathbf{e}_{1:n}^{(i)})} \right) \right).$$

Note that  $S_{1:k}^{(n)}$  is not a Markov process and indeed the jumping rates depend also on the last  $(n-k)$  components  $(x_{k+1}, \dots, x_n)$ . We now show that, given  $R_n^{(k)}$  as in Lemma 3, it holds

$$\sup_{\mathbf{x}_{1:n} \in \{0,1\}^k \times R_n^{(k)}, \mathbf{y}_{1:k} \in \{0,1\}^k} |A^{(n)}(\mathbf{x}_{1:k}, \mathbf{y}_{1:k}) - A(\mathbf{x}_{1:k}, \mathbf{y}_{1:k})| \xrightarrow{n \rightarrow \infty} 0. \quad (37)$$

Equation (37), together with  $\lim_{n \rightarrow \infty} \pi^{(n)}(\{0,1\}^k \times R_n^{(k)}) = 1$  from Lemma 3, implies that that  $S_{1:k}^{(n)} \xrightarrow{n \rightarrow \infty} S_{1:k}$ , using Corollary 8.7 from Ethier and Kurtz, 1986, Ch.4. Suppose first  $x_i = 0$ . In this case it holds

$$|A^{(n)}(\mathbf{x}_{1:k}, \mathbf{x}_{1:k} + \mathbf{e}_{1:k}^{(i)}) - A(\mathbf{x}_{1:k}, \mathbf{x}_{1:k} + \mathbf{e}_{1:k}^{(i)})| = v_i(1-p_i) \left| \frac{1}{\frac{Z_g^{(n)}(\mathbf{x}_{1:n})}{n}} \left( c_i \wedge \left( (1-c_i) \frac{Z_g^{(n)}(\mathbf{x}_{1:n})}{Z_g^{(n)}(\mathbf{x}_{1:n} + \mathbf{e}_{1:n}^{(i)})} \right) \right) - \frac{c_i \wedge (1-c_i)}{\bar{Z}} \right|.$$

Adding and subtracting  $\frac{(c_i \wedge (1-c_i))}{\frac{Z_g^{(n)}(\mathbf{x}_{1:n})}{n}}$ , and using  $(1-p_i) \leq 1$ , the latter expression is upper bounded by

$$v_i \left( \frac{1}{\frac{Z_g^{(n)}(\mathbf{x}_{1:n})}{n}} \left| \left( c_i \wedge \left( (1-c_i) \frac{Z_g^{(n)}(\mathbf{x}_{1:n})}{Z_g^{(n)}(\mathbf{x}_{1:n} + \mathbf{e}_{1:n}^{(i)})} \right) \right) - (c_i \wedge (1-c_i)) \right| + \left| \frac{(c_i \wedge (1-c_i))}{\frac{Z_g^{(n)}(\mathbf{x}_{1:n})}{n}} - \frac{(c_i \wedge (1-c_i))}{\bar{Z}} \right| \right). \quad (38)$$

Defining  $\alpha_n = \frac{1}{n^{1/4}} + \left| \mathbb{E} \left[ \frac{Z_g^{(n)}(\mathbf{X}_{1:n})}{n} \right] - \bar{Z} \right|$ , so that  $\left| \frac{Z_g^{(n)}(\mathbf{x}_{1:n})}{n} - \bar{Z} \right| \leq \alpha_n$ , the expression in (38) is in turn bounded by

$$(\sup_{i \in \mathbb{N}} v_i) \left( \frac{1}{\bar{Z} - \alpha_n} \left| \frac{2\alpha_n}{\bar{Z} - \alpha_n} \right| + \left| \frac{\alpha_n}{\bar{Z}(\bar{Z} - \alpha_n)} \right| \right). \quad (39)$$

The case  $x_i = 1$  is analogous. The expression in (39) does not depend on  $\mathbf{x}_{1:n}$  and converges to 0 as  $n$  increases because  $\lim_{n \rightarrow \infty} \alpha_n = 0$ . Thus (37) holds as desired and  $S_{1:k}^{(n)} \xrightarrow{n \rightarrow \infty} S_{1:k}$ .  $\square$

**A.5.1 Some references for mixing time of product chains** For each  $k \in \mathbb{N}$ ,  $S_{1:k}$  is a continuous time Markov chain with independent components. Such chains are often called product chains and received considerable attention, for example in the context of the *cutoff* phenomenon (see e.g. Diaconis and Saloff-Coste [1996, Thm.2.9] or Levin et al. [2009, Ch.20.4] and references therein). In particular Levin et al. [2009, Thm.20.7], Barrera et al. [2006, Prop. 7] and Bon and Păltănea [2001, Cor. 4.3] provide results concerning the mixing time of  $\{S_{1:k}\}_{k=1}^{\infty}$ . Such results tell us that, in the case of a sequence of independent binary Markov processes like  $\{S_{1:k}\}_{k=1}^{\infty}$ , the asymptotic mixing time depends on the flipping rates of the worst components (provided they are a non-negligible quantity), and in particular in our case the mixing time is minimized by maximizing the quantity  $\bar{Z}(\mathbf{v})^{-1} \liminf_{i \rightarrow \infty} v_i$  (see Theorem 4 for the definition of  $\bar{Z}(\mathbf{v})$  and Barrera et al. [2006] and Bon and Păltănea [2001] for the precise assumptions on the flipping rates). It can be seen that the latter quantity is maximized by choosing  $v_i$  to be constant over  $i$ , meaning  $v_i = \bar{v}$  for any  $i \in \mathbb{N}$  for some  $\bar{v} > 0$ .

## B Supplement for the simulation studies

**B.1 Supplement to Section 6.2** Figure 8 provides additional traceplots, acceptance rates and effective sample sizes related to the simulation study in Section 6.2. Considering

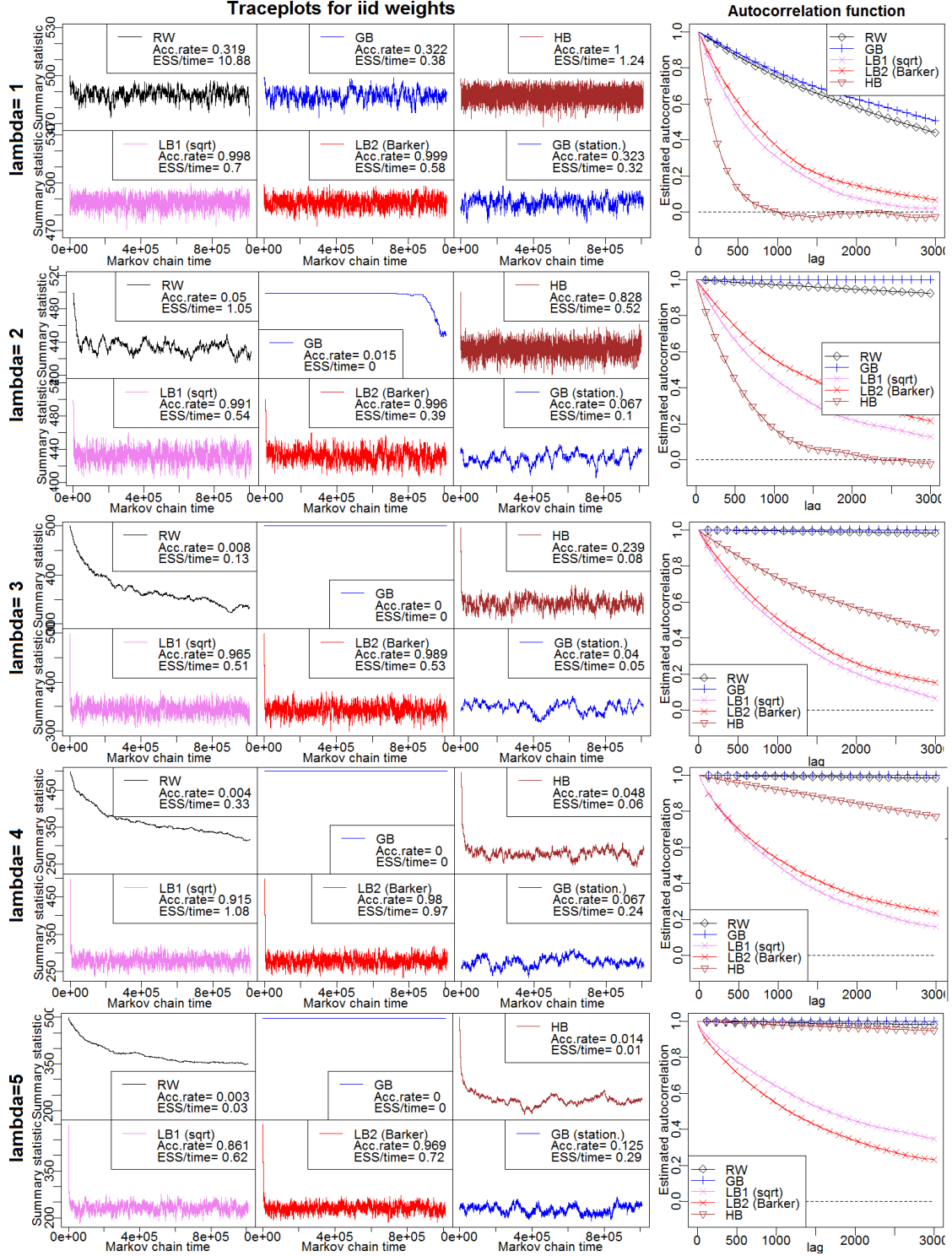


Figure 8: Performances for the five MCMC of Section 6.2 with targets as in Example 2,  $n = 500$  and  $\log(w_{ij}) \stackrel{iid}{\sim} N(0, \lambda^2)$ . Left: traceplots of a summary statistic (Hamming distance from fixed permutation). Right: estimated autocorrelation functions.

effective sample sizes per unit of computation time as measure of efficiency, it can be seen that the uninformed RW proposal performs best for flatter targets (i.e. small values of  $\lambda$ ), while as the roughness of the target increases (i.e. larger values of  $\lambda$ ) locally-balanced schemes strongly outperforms other schemes under consideration. Note that HB performs slightly better than locally-balanced schemes for flatter targets, but collapses as the target becomes more challenging.

**B.2 Supplement to Section 6.3** In Section 6.3 we tested the MCMC schemes under consideration using Ising model distributions as a benchmark. In particular we considered distributions motivated by Bayesian image analysis. In this context the variables  $x_i$  represent the classification of pixel  $i$  as “object” ( $x_i = 1$ ) or “background” ( $x_i = -1$ ). In a more general multiple-objects context one would use the Potts model, which is the direct generalization of the Ising model to variables  $x_i$ ’s taking values in  $\{0, 1, \dots, k\}$  for general  $k$ . Given the allocation variables  $\{x_i\}_{i \in V_n}$ , the observed image’s pixels  $\{y_i\}_{i \in V_n}$  are conditionally independent and follow a mixture model  $p(y_i | \{x_j\}_{j \in V_n}, \{y_j\}_{j \in V_n, j \neq i}) = p(y_i | x_i)$  where  $p(y_i | x_i = -1)$  is a distribution specific to background pixels and  $p(y_i | x_i = 1)$  is specific to object’s ones. For example  $p(y_i | x_i = -1)$  and  $p(y_i | x_i = 1)$  could be Gaussian distributions with parameters  $(\mu_{-1}, \sigma_{-1}^2)$  and  $(\mu_1, \sigma_1^2)$  respectively (see e.g. Moores et al. [2015a]). The allocation variables  $\{x_i\}_{i \in V_n}$  are given an Ising-type prior  $p(\{x_i\}_{i \in V_n}) \propto \exp(\lambda \sum_{(i,j) \in E_n} x_i x_j)$  to induce positive correlation among neighboring  $x_i$ ’s. It is easy to see that the resulting posterior distribution  $p(\{x_i\}_{i \in V_n} | \{y_i\}_{i \in V_n})$  follows an Ising model as in (9) with biasing terms  $\alpha_i$  given by  $\frac{1}{2} \log \left( \frac{p(y_i | x_i = 1)}{p(y_i | x_i = -1)} \right)$ .

In Section 6.3 we considered  $n \times n$  grids, with  $n$  ranging from 20 to 1000, and five levels of “concentration” for the target distribution. The latter are obtained by considering an increasing spatial correlation ( $\lambda = 0, 0.5, 1, 1, 1$ ) and an increasingly informative external field  $\{\alpha_i\}_{i \in V_n}$ . The external fields are illustrated in Figure 9. The object is at the center

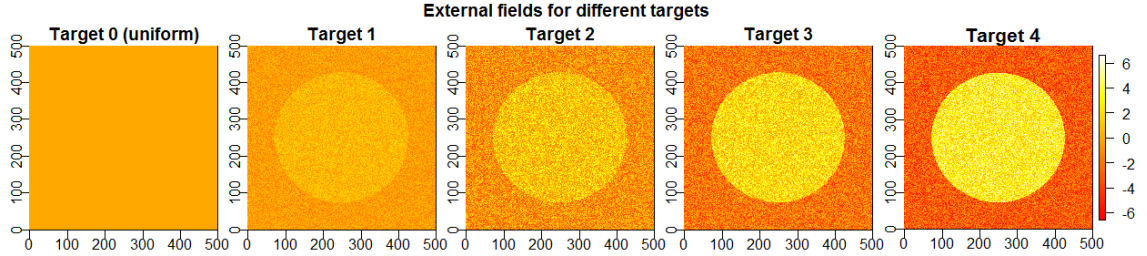


Figure 9: External fields  $\{\alpha_i\}_{i \in V_n}$  for the 5 different targets considered in Section 6.3. Here  $n = 500$ .

of the grid with a circular shape. If  $i$  is an object pixel we set  $\alpha_i = \mu + Z_i$ , while if it is a background pixel we set  $\alpha_i = -\mu + Z_i$ , where  $Z_i$  are iid  $Unif(-\sigma, \sigma)$  noise terms. For Target 0 up to Target 4 we considered  $\mu = 0, 0.5, 1, 2, 3$  and  $\sigma = 0, 1.5, 3, 3, 3$ . Note that Target 0 coincides with a uniform distribution on  $\{-1, 1\}^{n^2}$ , i.e.  $n^2$  i.i.d. Bernoulli random variables, where all schemes collapse to the same transition kernel. Figures 10 report traceplots, acceptance rates, effective sample sizes per unit time and autocorrelation functions for the five MCMC schemes for Targets 1-4.

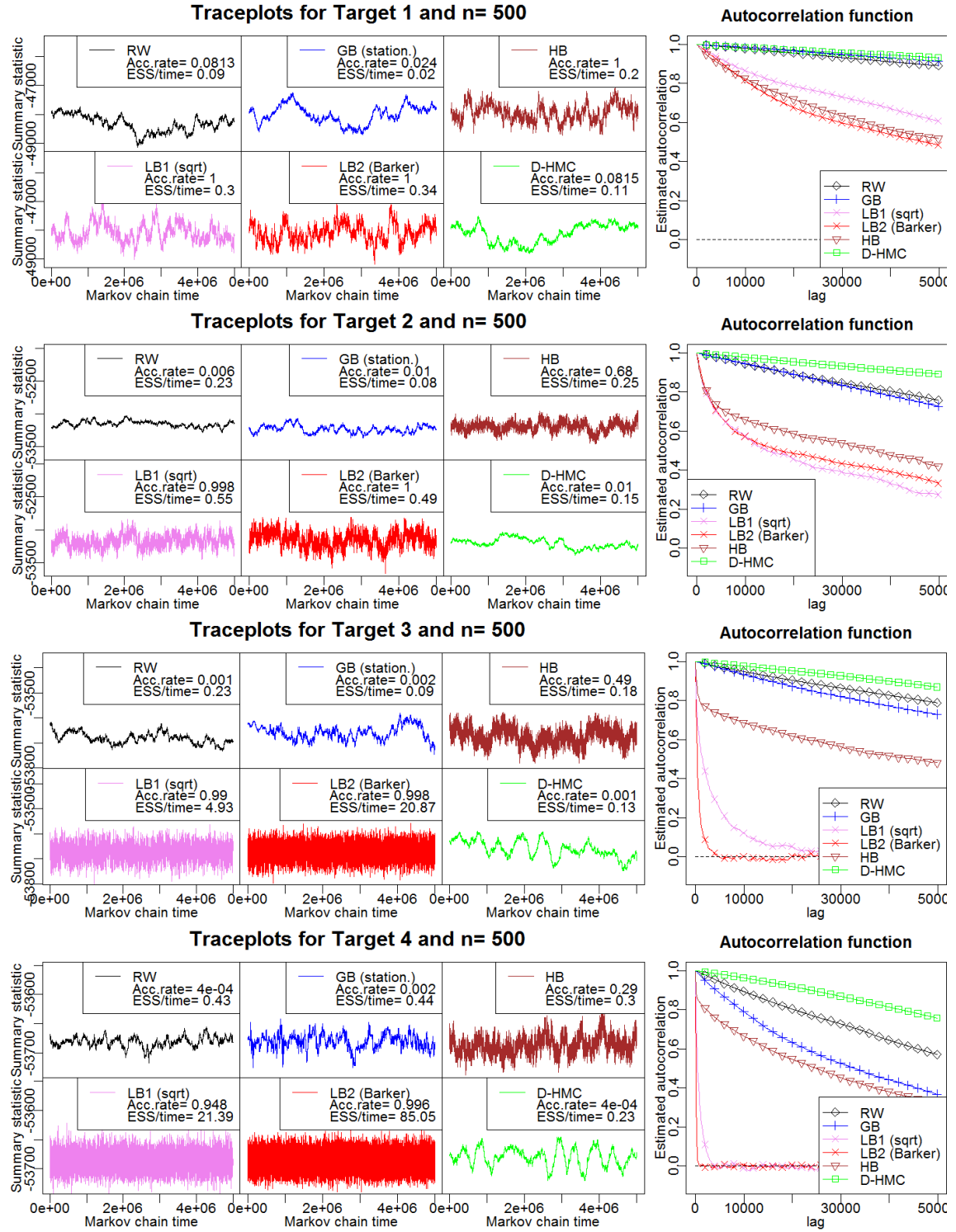


Figure 10: Performances for the six MCMC under comparison in Section 6.3 with target distributions described in Section B.2. For D-HMC we are plotting the whole trajectory, including the path during the integration period. Left: traceplots of a summary statistic (Hamming distance from fixed permutation). Right: estimated autocorrelation functions.

## C Supplement for the Record Linkage application

In this Supplement we describe in more details the Bayesian model for record linkage used in Section 7. The prior distribution follows mostly Miller et al. [2015] and Zanella et al. [2016], while the likelihood distribution is similar to, e.g. Copas and Hilton [1990] or Steorts et al. [2016]. The parameter of interest is the matching  $\mathbf{M} = (M_1, \dots, M_{n_1})$ , while the data are  $\mathbf{x} = (x_1, \dots, x_{n_1})$  and  $\mathbf{y} = (y_1, \dots, y_{n_2})$ .

**C.1 Prior distribution on the matching structure** We first specify a prior distribution for  $\mathbf{M}$ , which is the unknown matching between  $\{1, \dots, n_1\}$  and  $\{1, \dots, n_2\}$ . First, we assume the prior distribution of  $\mathbf{M}$  to be invariant with respect to permutations of  $\{1, \dots, n_1\}$  and  $\{1, \dots, n_2\}$ . This is a standard a priori assumption which is appropriate when the ordering of  $\mathbf{x}$  and  $\mathbf{y}$  is expected to carry no specific meaning. We then assume that the total number of entities in  $\mathbf{M}$  (i.e. number of matched pairs plus number of singletons) follows a Poisson distribution a priori with unknown mean  $\lambda$ . Given the number of entities, each of them either generates two records (one in  $\mathbf{x}$  and one in  $\mathbf{y}$ ) with probability  $p_{match}$  or otherwise generates a single record (which is assigned either to  $\mathbf{x}$  or to  $\mathbf{y}$  with equal probability). Both  $\lambda$  and  $p_{match}$  are treated as unknown hyperparameters. Such prior distribution for  $\mathbf{M}$  can be seen as a simple, bipartite version of the more general priors for Bayesian record linkage discussed in Zanella et al. [2016]. Note that also the sizes of  $\mathbf{x}$  and  $\mathbf{y}$ , which we denote by  $N_x$  and  $N_y$  respectively, are random objects a priori to be conditioned on the observed values  $n_x$  and  $n_y$ . The resulting prior distribution for  $\mathbf{M}$  given  $\lambda$  and  $p_{match}$  is

$$P(\mathbf{M}|\lambda, p_{match}) = \frac{e^{-\lambda} \lambda^{N_x + N_y - N_m}}{N_x! N_y!} \left( \frac{1 - p_{match}}{2} \right)^{N_x + N_y - 2N_m} p_{match}^{N_m}, \quad (40)$$

where  $N_m$  denotes the number of matches in  $\mathbf{M}$ .

*Derivation of (40).* First decompose the distribution of  $\mathbf{M}$  as

$$P(\mathbf{M}|\lambda, p_{match}) = P(\mathbf{M}|N_m, N_x, N_y) P(N_m, N_x, N_y|\lambda, p_{match}).$$

By the exchangeability assumption,  $P(\mathbf{M}|N_m, N_x, N_y)$  is simply one over the number of partial matchings between  $N_x$  and  $N_y$  indices with  $N_m$  matched pairs, i.e.

$$P(\mathbf{M}|N_m, N_x, N_y) = \binom{N_x}{N_m}^{-1} \binom{N_y}{N_m}^{-1} \frac{1}{N_m!} = \frac{N_m! (N_x - N_m)! (N_y - N_m)!}{N_x! N_y!}.$$

The expression for  $P(N_m, N_x, N_y|\lambda, p_{match})$  can be easily computed as

$$P(N_m, N_x, N_y|\lambda, p_{match}) = \frac{e^{-\lambda} \lambda^{N_x + N_y - N_m} \left( \frac{1 - p_{match}}{2} \right)^{N_x + N_y - 2N_m} p_{match}^{N_m}}{(N_x - N_m)! (N_y - N_m)! N_m!}.$$

noting that, given  $\lambda$  and  $p_{match}$ , the three random variables  $N_m$ ,  $N_x - N_m$  and  $N_y - N_m$  follow independent Poisson distributions with intensities  $\lambda p_{match}$  for the first and  $\lambda \left( \frac{1 - p_{match}}{2} \right)$  for the last two. Combining the previous expressions we obtain (40).  $\square$

For the purpose of the simulation studies in Section 7 we put independent, weakly informative priors on  $p_{match}$  and  $\lambda$ , such as  $\lambda \sim \text{Unif}([N_1 \vee N_2, N_1 + N_2])$  and  $p_{match} \sim \text{Unif}([0, 1])$ .

**C.2 Likelihood distribution** The distribution of  $(\mathbf{x}, \mathbf{y})|\mathbf{M}$  follows a discrete spike and slab model, also known as hit and miss model in the record linkage literature [Copas and Hilton, 1990]. The observed data consist of two lists  $\mathbf{x} = (x_i)_{i=1}^{n_x}$  and  $\mathbf{y} = (y_j)_{j=1}^{n_y}$ , where each element  $x_i$  and  $y_j$  contains  $\ell$  fields, i.e.  $x_i = (x_{is})_{s=1}^\ell$  and  $y_j = (y_{js})_{s=1}^\ell$ . Each field  $s \in \{1, \dots, \ell\}$  has a specific number of categories  $m_s$  and density vector  $\boldsymbol{\theta}_s = (\theta_{sp})_{p=1}^{m_s}$ . In real data applications, we assume  $\boldsymbol{\theta}_s$  to be known and estimate it with the empirical distribution of the observed values of the  $s$ -th field. This is a standard empirical bayes procedure typically used for this kind of models (see e.g. Zanella et al. [2016]).

Entities are assumed to be conditionally independent given the matching  $\mathbf{M}$ . If a datapoint, say  $x_i$ , is a singleton, then each field value  $x_{is}$  is drawn from  $\boldsymbol{\theta}_s$

$$x_{is} \sim \boldsymbol{\theta}_s \quad s \in \{1, \dots, \ell\},$$

and similarly for singletons  $y_j$ . If instead  $x_i$  and  $y_j$  are matched to each other, first a common value  $v_s$  is drawn from  $\boldsymbol{\theta}_s$  for each field  $s$  and then, given  $v_s$ ,  $x_{is}$  and  $y_{js}$  are independently sampled from a mixture of  $\boldsymbol{\theta}_s$  and a spike in  $v_s$

$$x_{is}, y_{js} | v_s \stackrel{iid}{\sim} \beta \boldsymbol{\theta}_s + (1 - \beta) \delta_{v_s} \quad s \in \{1, \dots, \ell\},$$

where  $\beta$  is a distortion probability in  $(0, 1)$ . In principle one would like to include the distortion probability  $\beta$  in the Bayesian model as an unknown hyperparameter. However, the latter is a difficult parameter to estimate in this contexts and previous Bayesian works in this context required very strong prior information (see e.g. the discussion in Steorts [2015]). For simplicity, in our context we assume  $\beta$  to be known and we set it to 0.001 which is a realistic value for the Italy dataset according to the discussion in Steorts [2015]. We ran simulations for different values of  $\beta$  (e.g. 0.01, 0.005, 0.002) and the results regarding relative efficiency of the algorithms under consideration were consistent with the ones reported in Section 7. Finally, we obtain the following expression for the likelihood function

$$P(\mathbf{x}, \mathbf{y} | \mathbf{M}) = \left( \prod_{s=1}^{\ell} \left( \prod_{i=1}^{n_x} \theta_{sx_{is}} \right) \left( \prod_{j=1}^{n_y} \theta_{sy_{js}} \right) \right) \prod_{s=1}^{\ell} \prod_{i: M_i > 0} \left( \beta(2 - \beta) + \frac{(1 - \beta)^2}{\theta_{sx_{is}}} \mathbb{1}(x_{is} = y_{M_{is}}) \right), \quad (41)$$

where  $\{i : M_i > 0\}$  is the set of indices  $i \in \{1, \dots, n_x\}$  that are matched to some  $j \in \{1, \dots, n_y\}$ .

*Derivation of (41).* The conditional independence over fields and datapoints that are not matched implies that  $P(\mathbf{x}, \mathbf{y} | \mathbf{M})$  can be factorized as

$$\prod_{s=1}^{\ell} \left( \left( \prod_{i=1}^{n_x} \theta_{sx_{is}} \right) \left( \prod_{j=1}^{n_y} \theta_{sy_{js}} \right) \left( \prod_{i: M_i > 0} \frac{P(x_{js}, y_{M_{is}} | \mathbf{M})}{\theta_{sx_{is}} \theta_{sy_{M_{is}}}} \right) \right).$$

The term  $\frac{P(x_{js}, y_{M_{is}} | \mathbf{M})}{\theta_{sx_{is}} \theta_{sy_{M_{is}}}}$  equals

$$\sum_{p=1}^{m_s} \theta_{sp} \frac{(\beta \theta_{sx_{is}} + (1 - \beta) \mathbb{1}(x_{is} = p))}{\theta_{sx_{is}}} \frac{(\beta \theta_{sy_{js}} + (1 - \beta) \mathbb{1}(y_{js} = p))}{\theta_{sy_{M_{is}}}}.$$

With simple calculations one can see that, if  $x_{is} = y_{M_{is}}$  the expression above equals  $\beta(2 - \beta) + \frac{(1 - \beta)^2}{\theta_{sx_{is}}}$ , while if  $x_{is} \neq y_{M_{is}}$  it equals  $\beta(2 - \beta)$ . Combining the latter equations we obtain (41).  $\square$



**C.3 Metropolis-within-Gibbs sampler** We use a Metropolis-within-Gibbs scheme to sample from the posterior distribution of  $(\mathbf{M}, \lambda, p_{\text{match}}) | (\mathbf{x}, \mathbf{y})$ . The two hyperparameters  $\lambda$  and  $p_{\text{match}}$  are conditionally independent given  $(\mathbf{x}, \mathbf{y}, \mathbf{M})$ , with full conditionals given by

$$p_{\text{match}} | \mathbf{x}, \mathbf{y}, \mathbf{M} \sim \text{Beta}(1 + n_x + n_y - 2N_m, 1 + N_m), \quad (42)$$

$$\lambda | \mathbf{x}, \mathbf{y}, \mathbf{M} \sim \text{Gamma}_{[\min\{n_x, n_y\}, n_x + n_y]}(1 + n_x + n_y - N_m, 1), \quad (43)$$

where  $N_m$  is the number of matched pairs in  $\mathbf{M}$  and  $\text{Gamma}_{[a,b]}$  denotes a Gamma distribution truncated on the interval  $[a, b]$ . The full conditional distribution of  $\mathbf{M}$  is proportional to

$$P(\mathbf{M} | \mathbf{x}, \mathbf{y}, \lambda, p_{\text{match}}) \propto \prod_{i: M_i > 0} \left( \frac{4p_{\text{match}}}{\lambda(1 - p_{\text{match}})^2} \prod_{s=1}^{\ell} \left( \beta(2 - \beta) + \frac{(1 - \beta)^2}{\theta_{sx_{is}}} \mathbb{1}(x_{is} = y_{M_{is}}) \right) \right). \quad (44)$$

The Metropolis-within-Gibbs scheme alternates Gibbs updates for  $p_{\text{match}}$  and  $\lambda$  according to (42) and (43) with Metropolis updates for  $\mathbf{M}$  according to (44). The challenging and computationally intense step is updating  $\mathbf{M}$  in an effective way and that's where we compare different sampling schemes (see Section 7). The four sampling schemes we compare (denoted by RW, GB, LB and HB) are all based on the same base kernel  $K(\mathbf{M}, \mathbf{M}')$ , which proceed as follows. First a couple  $(i, j)$  is sampled uniformly at random from  $\{1, \dots, n_x\} \times \{1, \dots, n_y\}$ . Then, given  $\mathbf{M}$  and  $(i, j)$ , one of the following moves is performed:

- Add move: if  $M_i = 0$  and  $M_j^{-1} = 0$ , set  $M_i = j$ ;
- Delete move: if  $M_i = j$ , set  $M_i = 0$ ;
- Single switch move (I): if  $M_i = 0$  and  $M_j^{-1} = i'$  for some  $i' \in \{1, \dots, n_x\}$ , set  $M_i = j$  and  $M_{i'} = 0$ ;
- Single switch move (II): if  $M_i = j'$  for some  $j' \in \{1, \dots, n_y\}$  and  $M_j^{-1} = 0$ , set  $M_i = j$ ;
- Double switch move: if  $M_i = j'$  for some  $j' \in \{1, \dots, n_y\}$  and  $M_j^{-1} = i$  for some  $i' \in \{1, \dots, n_x\}$ , set  $M_i = j$  and  $M_{i'} = j'$ .

Here  $M_j^{-1}$  is defined as  $M_j^{-1} = i$  if  $i$  is currently matched with  $j$  and  $M_j^{-1} = 0$  if no index is matched to  $j$ .

**C.4 Blocking implementation** In this context, sampling from GB, LB and HB has a computational cost that grows with  $n_x$  and  $n_y$ . When the latter terms are too large, it is more efficient to apply informed schemes to sub-blocks of indices (see discussion in Section 6.4). In Section 7 we used the following block-wise implementation:

1. choose a subset of indices  $I \subset \{1, \dots, n_x\}$  and a subset  $J \subset \{1, \dots, n_y\}$  (details below)
2. remove the indices  $i \in I$  that are matched with some  $j \notin J$  and, similarly, remove the indices  $j \in J$  that are matched with some  $i \notin I$
3. update the components  $(M_i)_{i \in I}$  by performing  $k$  iterations of the MCMC kernel under consideration restricting the proposal of couples  $(i, j)$  to  $I \times J \subseteq \{1, \dots, n_x\} \times \{1, \dots, n_y\}$ .

Step 2 is needed to avoid moves that would involve indices outside  $I \times J$ . It is easy to check that, if the MCMC used on the  $I \times J$  subspace is invariant with respect to  $\prod_{i \in I} w_{iM_i}$ , then the whole chain is invariant with respect to  $\prod_{i=1}^{n_x} w_{iM_i}$ . There are many valid ways to choose the subsets  $I$  and  $J$  in Step 1 (both randomly and deterministically). In our implementation in Section 7 we set the size of  $I$  and  $J$  to 300. In order to favour couples

having a non-negligible probability of being matched we alternated a uniformly at random selection of  $I$  and  $J$  (which ensures irreducibility) with the following procedure: sample an index  $i_0 \in \{1, \dots, n_x\}$  and three features  $\{s_1, s_2, s_3\} \subseteq \{1, \dots, \ell\}$  uniformly at random; define  $I$  and  $J$  as the set of  $i$ 's and  $j$ 's such that  $x_i$  and  $y_j$  respectively agree with  $x_{i_0}$  on the three selected features; if the size of  $I$  or  $J$  exceeds 300, reduce it to 300 with uniform at random subsampling. We claim no optimality for the latter procedure and defer the detailed study of optimal block-wise implementations to further work (see Section 8).